Chapter

Prion Proteins and Neuronal Death in the Cerebellum

Audrey Ragagnin, Qili Wang, Aurélie Guillemain, Siaka Dole, Anne-Sophie Wilding, Valérie Demais, Cathy Royer, Anne-Marie Haeberlé, Nicolas Vitale, Stéphane Gasman, Nancy Grant and Yannick Bailly

Abstract

The cellular prion protein, a major player in the neuropathology of prion diseases, is believed to control both death and survival pathways in central neurons. However, the cellular and molecular mechanisms underlying these functions remain to be deciphered. This chapter presents cytopathological studies of the neurotoxic effects of infectious prions and cellular prion protein-deficiency on cerebellar neurons in wild-type and transgenic mice. The immunochemical and electron microscopy data collected in situ and ex vivo in cultured organotypic cerebellar slices indicate that an interplay between apoptotic and autophagic pathways is involved in neuronal death induced either by the infectious prions or by prion protein-deficiency.

Keywords: prion protein, Doppel, apoptosis, autophagy, cerebellum, mouse

1. Introduction

1.1 Prion diseases

Transmissible spongiform encephalopathies (TSEs) or "prion diseases" are fatal neurodegenerative disorders in humans (Creutzfeldt-Jakob disease (CJD), Gerstmann-Straüssler-Scheinker syndrome (GSS), variant CJD (vCJD), fatal familial insomnia (FFI) and kuru) and in animals (bovine spongiform encephalopathy (BSE), transmissible mink encephalopathy (TME), chronic wasting disease of cervids (CWD), camel prion disease (CPD), and scrapie of sheep and goats) [1–4]. Prevailing over a viral etiology, the conformational corruption of host-encoded cellular prion protein (PrP^{c}) by a pathogenic isoform (PrP^{TSE}) is now widely accepted as underlying prion transmission and pathogenesis in TSEs [5–7].

1.2 PrP^{c} functions

Prnp-knockout mice were generated in order to investigate the physiological functions of PrP^{c}. In either mixed C57BL/6 j x129/Sv(ev) (Zurich I, ZrchI, $Prnp^{ZH1/ZH1}$, [8]) or pure 129/Ola (Npu, Edinburgh, Edbg, [9]) or C57BL/6J (Zurich III, ZrchIII, $Prnp^{ZH3/ZH3}$, [10]) genetic backgrounds, the first *Prnp* null

mouse strains produced were viable with no clear abnormality except for their resistance to prion infection [11] and absence of obvious neurodegeneration. Similar absence of neurodegeneration or histopathology resulted from depletion of neuronal PrP^c in adult conditional *Prnp*-knockout NFH-Cre/tg37 mice [12]. Thus, a physiological function of PrP^c that is essential for life seemed to be ruled out unless it is highly redundant or is compensated. Nevertheless, looking at different neuronal and other cell functions in PrP^c-ablated mice has revealed a number of differences that can be attributed to the physiological functions of PrP^c (see [13] for review).

PrP^c has been implicated in neurotransmission, olfaction, proliferation and differentiation of neural precursor cells, neuritic growth, neuronal homeostasis, cell signaling, cell adhesion, myelin maintenance, copper and zinc transport, as well as neuroprotection against toxic insults, such as oxidative stress and excitotoxicity (see [14, 15] for reviews). Increasing evidence links prion protein misfolding and accumulation to neurodegeneration in prion diseases. Accordingly, several nonexclusive mechanisms of prion-mediated neurotoxicity are currently under investigation (see [16] for review). PrP^c has been localized in three major sites: enriched in lipid rafts, anchored in the outer plasma membrane leaflet by its GPI tail [17], and intracellularly in the Golgi apparatus early and late endosomes [18, 19]. Since lipid rafts are pivotal microdomains for signal transduction, PrP^c is likely triggering intracellular signaling pathways [20, 21]. The first evidence that PrP^c might mediate extracellular signals was the caveolin-1-dependent coupling of PrP^c to the tyrosine-protein kinase Fyn [21]. From this pioneering work, accumulating data suggested that PrP^c functions as a "dynamic cell surface platform for the assembly of signaling molecules," partnering with other membrane proteins to transduce cellular signaling [22].

1.3 Synaptic PrP^c

Whereas, PrP^c is highly expressed in both neurons and glial cells of the CNS [19, 23, 24], it is preferentially localized in the pre- and postsynaptic terminals of neurons [19, 24, 25]. Immunocytochemical studies of primate and rodent brains [25, 26] including an EGFP-tagged PrP^c in transgenic mice, showed that PrP^c is enriched along axons and presynaptic terminals [27–29], and undergoes anterograde and retrograde transport [30, 31]. Such a synaptic targeting of PrP^c suggests that it could be involved in preserving synaptic structure and function. Indeed, synaptic dysfunction and loss are early prominent events in prion diseases [32, 33]. However, a functional role of PrP^c at synapses is not consistently supported by functional data and still remains contentious.

Insights into possible mechanisms by which PrP^c modulates synaptic mechanisms and neuronal excitability at a molecular level have been provided by the documented interactions of PrP^c with several ion channels including the voltage-gated calcium channels (VGCCs) [34], the N-methyl-D-aspartate glutamate receptors (NMDARs) [35] and the voltage-gated potassium channels Kv4.2 [36]. PrP^c has been shown to regulate NMDARs due to its affinity for copper that leads to inhibition of glutamate receptors and excitotoxicity [37, 38]. While interaction of PrP^c with these channels may account for some of its functions, a toxic response can also be activated when PrP^c misfolds. A structural change in cell surface PrP^c has been proposed to simultaneously disrupt NMDAR function and plasma membrane permeability, leading to dysregulation of ion homeostasis and neuronal death [39, 40]. PrP^c can also interact with kainate receptor subunits GluR6/7 [41], α-amino-3-hydroxy-5-methyl-4-isoxazolepropionic acid (AMPA) receptors subunits GluA1 and GluA2 [42, 43], and metabotropic glutamate receptors of group 1 mGluR1 and mGluR5 [44, 45]. PrP^c can interact with the β-amyloid peptide (Aβ) and the later [45, 46] is believed to underlie the Aβ

oligomer-induced disruption of LTP in Alzheimer's disease [47]. Thus, PrP^c seems to behave as a cell surface receptor for synaptic oligomers of the Aβ peptide and, of other β-sheet-rich neurotoxic proteins [40].

1.4 PrP^{TSE}-related neurotoxicity in prion diseases

The histopathological signature of TSEs notably relies on the aggregation of PrP^{TSE}, vacuolation of the brain tissue, astrogliosis, and synaptic and neuronal loss. How neurons, the major targets of prions, die, remains a central question in prion diseases. The absence of neurodegenerative phenotypes after depletion of PrP^c suggests that neurotoxicity is not due to a loss of PrP^c function but rather results from a gain of toxicity upon its conversion to PrP^{TSE}, which then acts on the central nervous system (CNS) [48]. Although PrP^c is required for propagation of infectious prions and PrP^{TSE}-mediated toxicity [49], the mechanisms by which prions are lethal for neurons remain mostly unknown. Nevertheless, the endogenous PrP^c conversion has been shown to cause neuronal dysfunction and death, rather than PrP^{TSE} itself which does not seem to be directly neurotoxic. A precise understanding of the factors leading to neurotoxicity in prion infections is crucial to developing targeted therapies and investigating the role of PrP^c in neurons should provide insight.

The conformational conversion of PrP^c begins on the neuronal surface, where PrP^c interacts with exogenous PrP^{TSE}, and then proceeds within endogenous compartments suggesting that neurotoxicity may be triggered by PrP^c misfolding both at the cell surface and inside the cell. In both acquired and genetic prion diseases, intracellular PrP^c misfolding would ultimately alter synaptic proteostasis, either through an indirect unfolded protein response (UPR)-mediated mechanism [50], likely arising either from an impairment of the neuronal ubiquitin-proteasome system (UPS) [51], or a direct interference with secretory trafficking of PrP^c-interacting cargoes [52]. Common features associated with prion infections include Ca^{2+} dysregulation, release of reactive oxygen species, and induction of endoplasmic-reticulum (ER) stress, which has been recently suggested as an important player in pathogenesis [53]. Prion-infected mice show brisk activation of the UPR and specifically of the PERK pathway, resulting in eIF2α phosphorylation and suppression of translational initiation. PERK inhibition protects mice from prion neurotoxicity, confirming an important pathogenic role of ER stress [50]. Since UPR activation and/or increased eIF2α-P levels as well as UPS impairment are commonly seen in prion disorders and in Alzheimer's and Parkinson's diseases, translational control, and UPS stimulation strategies may offer a common therapeutic opportunity to prevent synaptic failure and neuronal loss in protein misfolding diseases [51, 54].

1.5 Loss of PrP^c anti-inflammatory protective function in prion disease

A protective role of PrP^c against a noxious insult mediated by the pro-inflammatory cytokine tumor necrosis factor-α (TNFα) has recently been demonstrated [55]. The α-secretase activity mediated by the TNFα-converting enzyme (TACE) was impaired at the surface of Fukuoka and 22L scrapie prion-infected neurons. Furthermore, the activity of 3-phosphoinositide-dependent kinase-1 (PDK1) which inactivates phosphorylation and caveolin-1-mediated internalization of TACE is increased in scrapie-infected neurons. PDK1 was shown to be controlled by RhoA-associated coiled-coil containing kinases (ROCK) which favored the PrP^{TSE} production. In these neurons, exacerbated ROCK activity overstimulated PDK1 activity which canceled the neuroprotective α-cleavage of PrP^c by TACE α-secretase, physiologically precluding PrP^{TSE} production. Inhibition of ROCK lowered PrP^{TSE} in prion-infected cells as well as in the brain of prion-diseased mice which had

extended lifespans [56]. Indeed, the dysregulation of TACE resulted in PrP^{TSE} accumulation and reduced the shedding of TNFα receptor type 1 (TNFR1) from the neuronal plasma membrane. Inversely, inhibition of PDK1 *in vitro* promoted TACE localization at the plasma membrane, restoring TACE-dependent α-secretase activity and shedding of PrP^{c} and TNFR1, thereby attenuating PrP^{TSE}-induced neurotoxicity. Similarly, inhibition or siRNA-mediated silencing of PDK1 extended survival and reduced motor impairment of scrapie-diseased mice [55]. Mechanistically, PrP^{c} coupling to the NADPH oxidase-TACE α-secretase signaling pathway limits the sensitivity of recipient cells to TNFα by promoting TACE-mediated cleavage of TNFα receptors (TNFRs) and the release of soluble TNFRs. PrP^{c} expression was further shown to be necessary for maintaining TACE α-secretase at the plasma membrane and its TNFR shedding activity. The loss of PrP^{c} provoked TACE internalization, canceling TACE-mediated cleavage of TNFR. This rendered PrP^{c}-depleted cells and *Prnp*-knockout mice highly vulnerable to pro-inflammatory TNFα insult. Thus, abnormal trafficking and activity of TACE in prion diseases likely originates from a loss of PrP^{c} cytoprotective function [57].

Synaptolysis is believed to initiate the neurodegeneration arising after a decrease in depolarization-induced calcium transients that progressively impairs glutamate release [34]. However, although cytoskeletal disruption in dendritic spines plays a major role in neuronal dysfunction, neither changes in postsynaptic densities and presynaptic compartment nor disruption of afferent innervation have been systematically observed, suggesting that even at terminal stages of the disease neuronal loss may not result from deafferentation as previously proposed in the hippocampus and cerebellum of scrapie-infected mice [33, 58, 59]. Thus, neuronal vulnerability to pathological protein misfolding appears to be more strongly dependent than previously thought, on the structure and function of target neurons.

Recent investigations of scrapie pathogenesis in the mouse cerebellum revealed an early upregulation of tumor necrosis factor-α receptor type 1 (TNFR1), a key mediator of neuroinflammation at the membrane of astrocytes enveloping Purkinje cell (PC) excitatory synapses already at the preclinical stage of the disease before PrP^{22L} precipitation, GFAP astrogliosis, and PC death [59]. The contribution of perisynaptic astrocytes to prion pathogenesis through TNFR1 upregulation remains to be clarified and, although the cell types responsible for PrP^{22L} production in the cerebellum are still uncertain, these data suggest a critical role for astrocytes in prion pathogenesis.

2. Mechanisms of neuronal death in prion diseases

Despite the overall advances made in this field during the last decades, the sequence of cellular and molecular events leading to neuronal cell demise in TSEs remains obscure. At present, neuronal cell death can be envisioned as resulting from several parallel, interacting, or sequential pathways involving protein processing and proteasome dysfunction [60], oxidative stress [61], inflammation [55] apoptosis, and autophagy [62]. The repertoire of pathways that lead to neuronal death is however limited [63]. In TSEs, apoptosis is the most popular theory of cell death but is not convincingly documented. In all cases, the probable disruption of both neuronal metabolism and circuits generates a pro-apoptotic signal for neurons. In addition to disruption of cellular proteostasis, UPS dysfunction may lead to neurotoxicity by activating pro-apoptotic pathways. PrP^{TSE} aggresomes can associate with pro-apoptotic factors such as vimentin and caspases [60]. On the other hand, autophagy has been reported in TSEs, but its role in prion disease pathology is not well established [64]. However, the extensive synaptic autophagy observed

in prion diseases [65] has been proposed to contribute to overall synaptic degeneration, a major precocious pathological feature leading to neuronal death in TSEs. This chapter reports recent biochemical and cytopathological studies investigating the involvement of apoptosis and autophagy in neuronal loss induced by infectious prions as well as by PrP^{c}-deficiency in the mouse cerebellum.

Among TSEs, scrapie is a natural ovine prion disease widely studied in mouse models using murine-adapted prion strains (22L, ME7) that, akin to natural prion strains, differ in their rate of disease progression (i.e., duration of the incubation period), as well as the extent and regional pattern of brain histopathology [66, 67]. For example, the characteristic of a prion strain mostly relies on specific biochemical properties related to PrP^{TSE} misfolding. The variable susceptibility of neuronal types to prion infection also emerges as another critical parameter that underlies the complex mechanisms of prion pathogenesis [54, 68, 69] and affects PrP^{TSE} progression along defined anatomical routes [70]. The cellular and molecular mechanisms involved in targeting PrP^{TSE} to specific neuronal populations [33, 71, 72] and neuron-to-neuron spreading of prions in the CNS remain elusive [73].

In several prion diseases, the cerebellum is a preferential prion target for scrapie [74–78], also observed in Creutzfeldt-Jakob disease (CJD) cases [79–87]. Cerebellar circuits are exquisitely patterned and the expression patterns of zebrins in PCs define a topographical map of genetically determined zones controlling sensory-motor behavior [88, 89]. Subsets of PCs expressing zebrins alternate with subsets of zebrin-free PCs, thus forming complementary stripes of biochemically distinct PCs [88]. The most comprehensively studied zonal marker is zebrin II/aldolase C (ZII/AldC) [90]. The expression of ZII/AldC by itself, however, is not sufficient to recapitulate the full complexity of the cerebellar cortex because of the many other PC subtypes [91, 92].

In a recent study [59], the parasagittal compartmentation of the cerebellar cortex restricted 22L scrapie pathogenesis, including PrP^{22L} accumulation, PC neurodegeneration, and gliosis. Indeed, PCs displayed a differential, subtype-specific vulnerability to 22L prions with zebrin-expressing PCs being more resistant to prion toxicity, whereas in stripes where PrP^{22L} accumulated most zebrin-deficient PCs were lost and spongiosis was accentuated (**Figure 1**). Although this banding pattern of PrP^{22L} accumulation is most likely delineated by structural constraints of compartmentation, different biochemical properties of PC subpopulations may well determine their differential resistance to scrapie prions.

2.1 Prion-induced apoptosis

2.1.1 Apoptotic pathways in prion-infected neurons

The mechanism of prion neurotoxicity requires neuronal expression of PrP^{c} and is based on the subversion of its normal function triggered by an interaction with PrP^{TSE} at the cell surface, thereby transducing a toxic signal into the cell. Nevertheless, this has been challenged by the discovery of a monomeric, highly α-helical form of PrP^{c} with strong *in vitro* and *in vivo* neurotoxicity that elicits autophagy and apoptosis with a molecular signature similar to that observed in prion-infected animal brains [93]. This toxic PrP (TPrP) killed PrP-deficient neurons *in vitro* suggesting that a PrP-derived toxic signal can be generated within neurons independently of endogenous membrane-bound PrP^{c}. Indeed, postnatal ablation of PrP^{c} expression in neurons reversed neurodegeneration and affected disease progression in mice even though glial replication was maintained and PrP^{TSE} accumulated [94]. Thus, prion pathogenesis is governed by both cell-autonomous mechanisms responsible for cellular dysfunction and neurodegeneration and noncellular-autonomous mechanisms propagating prion spread [95].

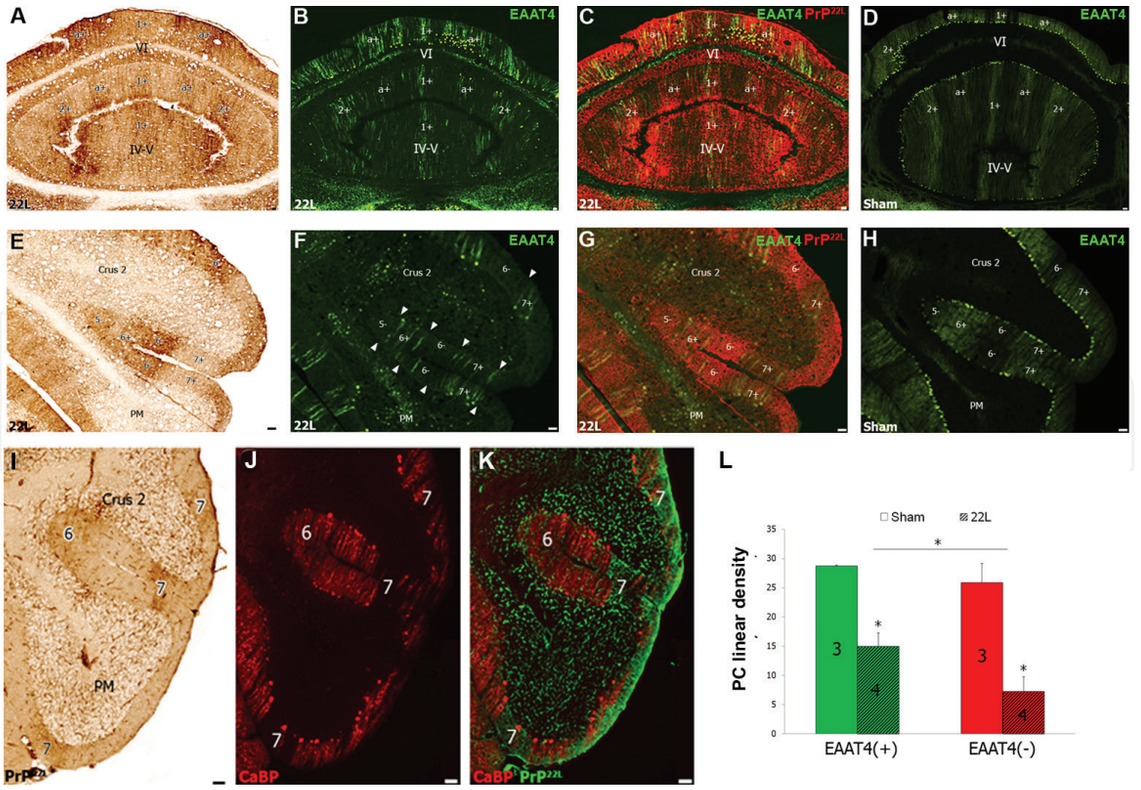

Figure 1.
Banding pattern of PrP^{22L}, EAAT4 zebrin and PC loss in the EAAT4-eGFP mouse cerebellum **A–H**. *The pattern of PrP^{22L} deposits (immunoperoxidase (immunoHRP) in A and E is artificially visualized in red in C and G) correlated with the banding pattern of the zebrin excitatory amino acid transporter 4 (EAAT4-eGFP, green in B, F) in merged PrP^{22L}-EAAT4 images C and G in the cerebellar vermis (A–C) and hemispheres (E–G) infected with 22L ic. (clinical stage 145 dpi). D, H. EAAT4-eGFP PCs in the same regions of the vermis (D) and hemisphere (H) of a noninfected EAAT4-eGFP mouse as shown in the cerebellum of the 22L-infected EAAT4-eGFP mouse (A–G). The zebrin bands are numbered according to the current nomenclature in A–K and indicated by arrowheads in F.* **I–K**. *In the cerebellum infected icb. (preclinical stage), two bands of PrP^{22L} deposits (6 and 7) are visualized by immunoHRP in I and artificially visualized in green in K. These cross crus2 and paramedian lobule (PM) and display a marked loss of CaBP-immunofluorescent PCs (red). Scale bars = 50 μm.* **L**. *Quantitative analysis of EAAT4-expressing and -nonexpressing PCs in the cerebellum of EAAT4-eGFP mice infected i.c. (clinical stage). The EAAT4-nonexpressing PCs are more sensitive to 22L toxicity. *$p < 0.05$. The number of mice analyzed is indicated on the bars in the graph.*

Endoplasmic-reticulum stress has recently been implicated in an apoptotic regulatory pathway activated by changes in Ca^{2+} homeostasis or accumulation of aggregated proteins. In both these situations, Ca^{2+} is released and caspase-12 is activated [96]. ER stress and caspase-12 activation have been identified in prion-infected N2a cells as well as in the brains of prion-diseased mice and CJD patients [97]. The synaptic dysfunction and neuronal death caused by PrP^{TSE} accumulation via dysregulation of the Ca^{2+}-sensitive phosphatase calcineurin (CaN) provides further evidence of the role of ER stress and Ca^{2+} homeostasis in prion-induced neurodegeneration [98]. The increase in Ca^{2+} cytosolic levels following hyperactivation of CaN dysregulates the pro-apoptotic Bcl-2-associated death promoter (Bad), and the transcription factor cAMP response element-binding (CREB). Dephosphorylated Bad interacts with Bax causing mitochondrial stress and apoptosis while dephosphorylated CREB cannot translocate into the nucleus to regulate the transcription of synaptic proteins, resulting in synaptic loss [99].

2.1.2 Mitochondrial apoptosis in prion-infected cerebellar neurons

PrP^{c} has recently been suggested to participate in anti-apoptotic and anti-oxidative processes by interacting with the stress inducible protein 1 (STI-1) to regulate superoxide dismutase (SOD) activation [100]. The PrP^{c} octapeptide repeat

region contains a B-cell-lymphoma 2 (Bcl-2) homology domain 2 (BH2) of the family of apoptosis regulating Bcl-2 proteins involved in the anti-apoptotic function of Bcl-2. A direct interaction between PrPc and the C-terminus of anti-apoptotic Bcl-2 has also been found [101, 102]. In addition, the third helix of PrP^{c} impaired the BAX conformation changes required for apoptosis activation suggesting that PrP^{c} may assure the neuroprotective function of Bcl-2 [103]. Along this line, $Prnp^{0/0}$ neurons were more susceptible to apoptotic stimuli such as serum deprivation than their wild-type counterparts, whereas they were rescued by PrP^{c} or Bcl-2 expression [104, 105]. PrP^{c} also protected primary neurons against BAX-dependent apoptosis. Furthermore, transgenic expression of *Bax* or *Bax* and *Prnp* indicated that *Prnp* impairs *Bax*-dependent neuronal death [106].

Activation of the mitochondrial apoptotic pathway was observed when primary neurons were exposed to aggregated neurotoxic peptides like PrP106-126 or recombinant mutant PrP [107–109]. Apoptotic neuronal death demonstrated by activation of several caspases and DNA fragmentation is evident in natural prion diseases as well as in experimental models of TSEs [76, 110, 111]. In the cerebellum, apoptotic features have been observed in granule cells in CJD patients [112, 113] as well as in mice experimentally infected with CJD [111] and scrapie strains 301V, 87V, 22A [76], 79A [110], M1000/Fukuoka-1 [114], 127S [115], 22L, 139A, and RML [116, 117]. More recently, activation of caspase-3 was found in PCs of 22L-infected mice [59]. However, cerebral upregulation of the pro-apoptotic factor BAX has been reported in some cases of scrapie-infected rodents [116, 118], whereas no changes in clinical illness and neuropathology could be detected in the brain of Bax-deficient mice infected with 6PB1 mouse-adapted BSE prions [119]. This suggested that BAX-mediated cell death is not involved in the pathological mechanism induced by BSE. Nevertheless, BAX is known to be involved in neuronal death in Tg(PG14) [120] and Ngsk $PrnP^{0/0}$ [121] murine models of PrP-deficiency-linked diseases. In these cases, neuronal death is restricted to cerebellar neurons that are known to undergo BAX and BCL2-dependent apoptosis in other abnormal conditions [122, 123]. This led us to further investigate the involvement of intrinsic mitochondrial apoptotic pathways in a cerebellotropic prion disease such as the 22L scrapie. For this purpose, the pathogenesis of 22L scrapie in the brain of *Bax*-KO ($Bax^{-/-}$) mice [124] and in mice expressing a human Bcl-2 transgene [125] was analyzed. Clinical signs of 22L scrapie (mainly ataxia) were similar to those previously described for C57Bl/6 mice [126]. $Bax^{-/-}$ and HuBcl-2 mice infected by either intraperitoneal (ip.) or intracerebellar (icb.) route displayed ataxia 10–15 days sooner than wild-type mice. Survival times however, were similar in all genotypes (i.e., 223 dpi ip. and 129 dpi icb.). whereas 22L induced more severe cerebellar spongiosis via the icb. route than the ip. route, similar lesion profiles [71] were induced by 22L ip. in the brain of $Bax^{-/-}$ and wild-type mice and lesion profiles were not different in the brain of $Bax^{-/-}$, HuBcl-2 and wild-type mice infected with 22L icb. (**Figure 2**). Anatomopathological analysis of the cerebral and cerebellar cortices of the 22L-diseased $Bax^{-/-}$ and HuBcl-2 mice did not reveal any modified patterns of vacuolation, astrogliosis, and PrP^{22L} deposits irrespective of the inoculation route. Synaptophysin and calcium-binding protein (CaBP) immunohistochemistry also revealed severe synapse and PC loss in all cases (**Figure 3**). Finally, quantitative analysis of the cerebellar granule cells immunolabeled for the nuclear marker NeuN revealed a significant loss of neurons in all genotypes infected by the icb. route (**Figure 4**). Surprisingly, no significant difference could be detected between $Bax^{-/-}$ and wild-type mice infected by the icb. route, whereas HuBcl-2 mice whose granule cells are rescued from developmental cell death [127] lost more granule cells than wild-type and $Bax^{-/-}$ mice (**Figure 4**). These data indicate that neither suppression of *Bax* nor overexpression of Bcl-2 protected cerebellar neurons from 22L scrapie-induced neurotoxicity. Thus, the granule cell

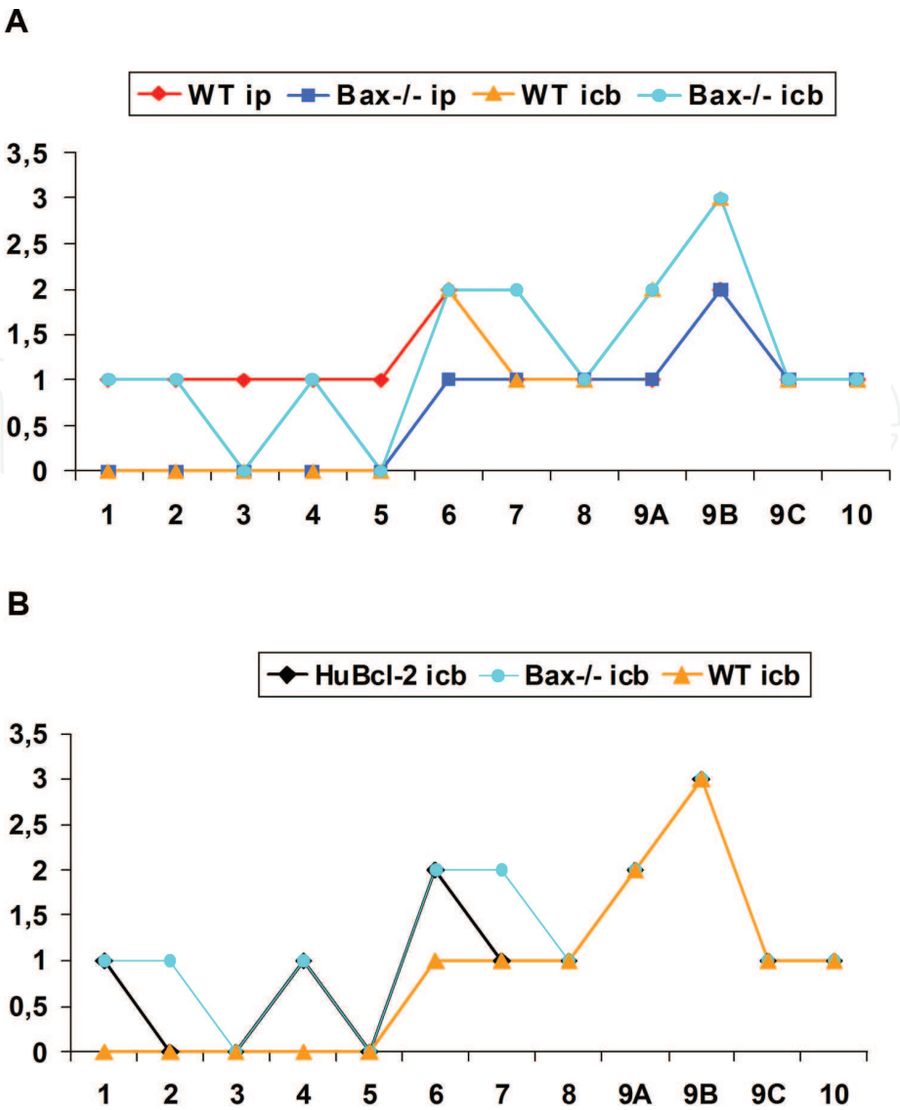

Figure 2.
Spongiosis lesion profiles in the brain of wild-type (WT), Bax$^{-/-}$ and HuBcl-2 mice infected ip. and icb. with the 22L scrapie prion strain. **A.** *Very similar lesion profiles were induced by 22L scrapie ip. in Bax$^{-/-}$ and WT mice. 22L induced more severe cerebellar spongiosis via the icb. route than via the ip. route. 1: cingulate and 2nd motor cortices, 2: lateral and medial septum, 3: caudate putamen, 4: retrosplenial cortex, 5: hippocampus, 6: thalamus, 7: hypothalamus, 8: superior colliculus, 9A: cerebellar molecular layer, 9B: cerebellar granular layer, 9C: cerebellar white matter, 10: medulla.* **B.** *Very similar lesion profiles were induced by 22L scrapie icb. in Bax$^{-/-}$, HuBcl-2 and WT mice.*

and PC death induced by 22L scrapie does not seem to involve BAX and cannot be counteracted by overexpression of the anti-apoptotic factor BCL-2. However, cleaved caspase-3 and -9 were observed in the brains of Bax$^{-/-}$ mice, suggesting that apoptosis may occur through (an) alternative mechanism(s) in TSEs of infectious origin. Indeed, apoptotic features have been reported in the brain of wild-type mice infected with RML, in the absence of Bax upregulation [116], while other proteins involved in cell death including those associated with the mitochondrial inner membrane, the UPS and the endoplasmic-reticulum-associated protein degradation (ERAD) pathway [128] were upregulated.

2.1.3 Prion-induced neuronal death in cerebellar organotypic slice cultures (COCS)

In the recently developed prion cerebellar organotypic slice culture (COCS) assay, progressive spongiform neurodegeneration that closely reproduce features of prion disease can be induced *ex vivo* [117, 129]. Infecting COCS with three different scrapie strains (RML, 22L, 139A) produced three distinct patterns of prion protein

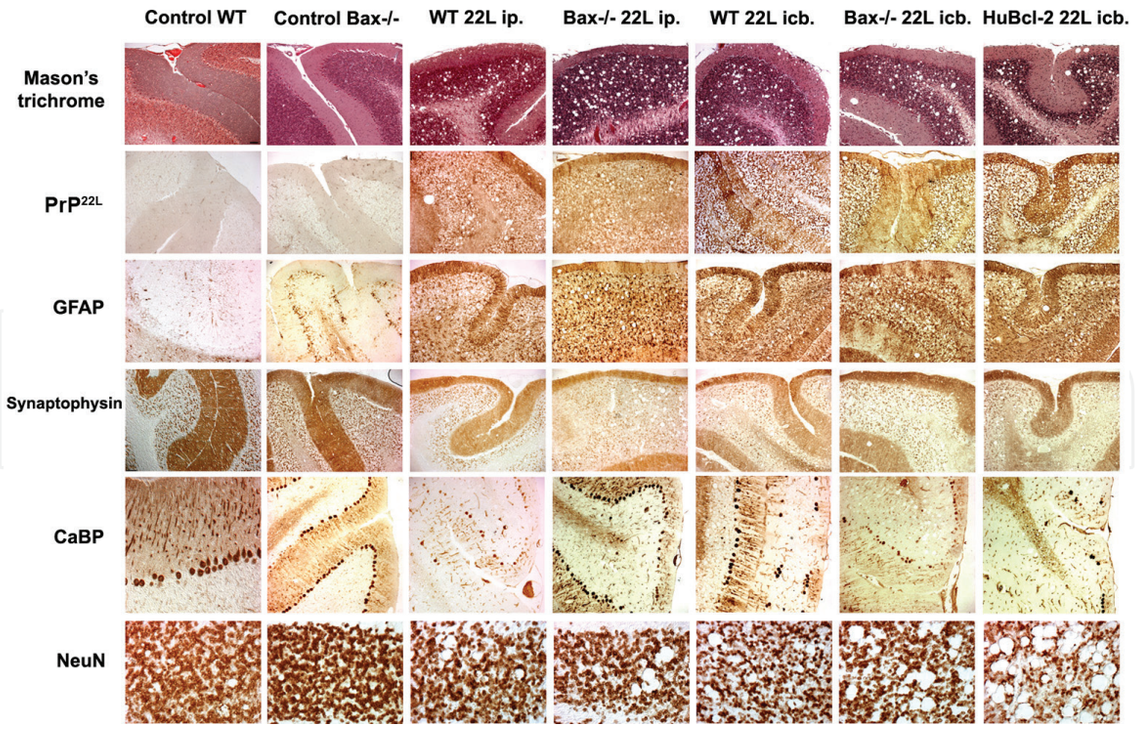

Figure 3.
Anatomopathology of 22L scrapie ip. and icb. in the cerebellum of WT, Bax$^{-/-}$ and HuBcl-2 mice. Neither Bax knockout nor HuBcl-2 overexpression modified vacuolation (Mason's trichrome), astrogliosis (GFAP immunoHRP) and PrP^{22L} accumulation (PrP immunoHRP) patterns in the cerebellar cortex of the 22L ip. and icb. infected Bax$^{-/-}$ and HuBcl-2 mice compared to the WT mice. Synaptophysin and CaBP reveal respectively synapse and PC loss in the cerebellum of all mice. Loss of Neun-immunostained GCs is also prominent in the cerebellum of the WT, Bax$^{-/-}$ and HuBcl-2 infected icb., yet seemed less pronounced in the mice infected ip.

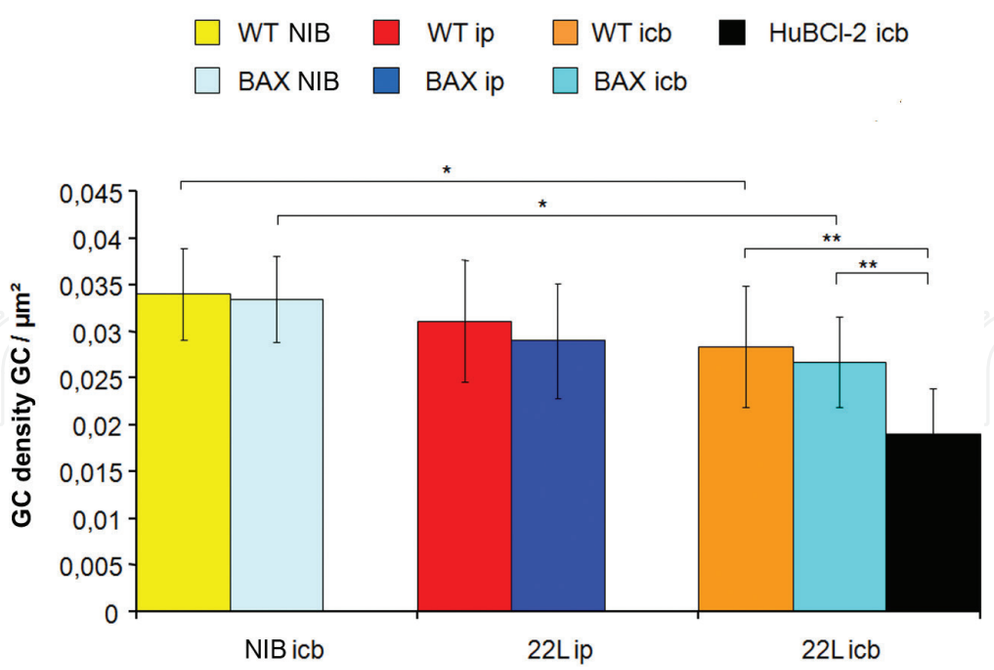

Figure 4.
*Quantitative analysis of cerebellar GCs immunostained for the nuclear marker NeuN revealed a significant loss of neurons in all genotypes infected icb., but not ip. *p < 0.05; **p < 0.01. Whereas Bax$^{-/-}$ and WT mice lost a similar amount of GCs, the HuBcl-2 mice lost more GCs than the WT and Bax$^{-/-}$ mice. NIB, noninfected brain homogenate.*

deposition accompanied by salient features of prion disease pathogenesis such as severe neuronal loss, a pro-inflammatory response, and typical neuropathological changes (spongiform vacuolation, tubulovesicular structures, neuronal dystrophy,

and gliosis). Neurodegeneration did not occur when PrP was genetically removed from neurons and was abrogated by compounds known to antagonize prion replication. Also, calpain inhibitors, but not caspase inhibitors, prevented neurotoxicity and fodrin cleavage; whereas, prion replication was unimpeded indicating that inhibiting calpain uncouples prion replication and neurotoxicity. These data validate the COCS as a powerful model system that faithfully reproduces many morphological hallmarks of prion infections and shows that prion neurotoxicity in cerebellar granule cells is calpain-dependent but caspase-independent.

Furthermore, significant spine loss and altered dendritic morphology, analogous to that seen *in vivo* were induced by RML scrapie in COCS [130], while the deposition pattern and subcellular distribution of PrP^{22L} (i.e., granular deposits associated with neurons, astrocytes, and microglia but not PCs in the neuropil of the PC and molecular layers [131]), closely resembled that observed *in vivo* [59].

Following infection of COCS from C57Bl6/J, ZH-I $Prnp^{0/0}$, and Tga20 PrP-overexpressing mice with brain homogenate from C57Bl6/J infected intracerebrally (ic.) with either 22L or 139A scrapie prions, PrP^{22L} and PrP^{139A} accumulation could be detected on histoblots from wild-type and Tga20 COCS, respectively, 30 and 20 days post infection (dpi), but not on histoblots from ZH-I mice (**Figure 5**). Furthermore, quantitative analysis of PCs in these COCs indicated that a severe loss of neurons was induced by 22L prions in wild-type slices at 30 dpi (22 ± 2 surviving PCs/slice) and in Tga20 slices at 20 dpi (293 ± 68 surviving PCs) as well as by 139A prions in wild-type slices at 30 dpi (145 ± 63 surviving PCs/slice) and in Tga20 slices at 20 dpi (191 ± 31 surviving PCs/slice) compared to noninfected control COCS (220 ± 27 surviving PCs/slice in wild-type slices and 357 ± 71 surviving PCs/slice in Tga20 slices) (**Figure 6**). At 30 dpi, the trilaminar organization of the cerebellar cortex was evident in noninfected COCs, which did not exhibit any clear ultrastructural modifications (**Figure 7**). Nevertheless, numerous vacuoles, autophagosomes, and lysosomes had formed in granule cells infected by 22L and 139A (**Figure 8**). In diseased PCs, autophagosomes with double membranes and rough endoplasmic reticulum (Nissl bodies) formed compartmented organelles of various sizes (1–10 compartments) resembling different stages leading to multivesicular vacuoles (**Figure 9**). Although further investigations are necessary, these ultrastructural

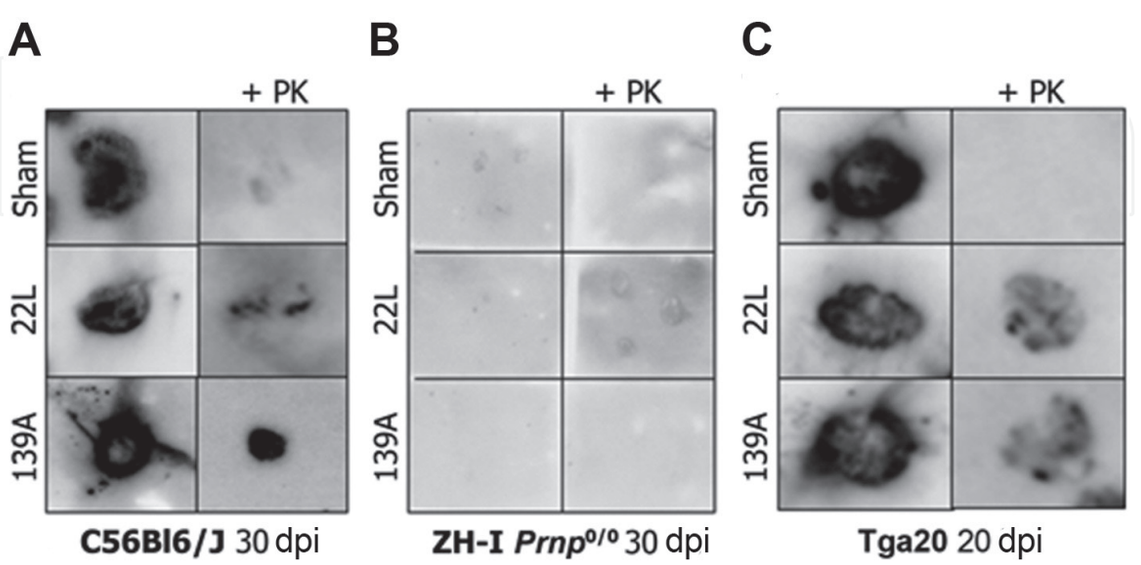

Figure 5.
Histoblots of cultured organotypic cerebellar slices (COCS) infected with the 22L and 139A scrapie strains. PrP^c was detected in histoblots of noninfected (sham) COCS from WT C57Bl6/J (A) and Tga20 PrP-overexpressing (C), but not PrP-deficient ZH-I $PrnP^{0/0}$ (B) mice. PrP^c was completely digested by proteinase K (PK) in these COCS. After 30 and 20 days postinfection (dpi), PK revealed undigested PrP^{22L} and PrP^{139A} respectively in the WT and Tga20, but not ZH-I $Prnp^{0/0}$ infected COCS.

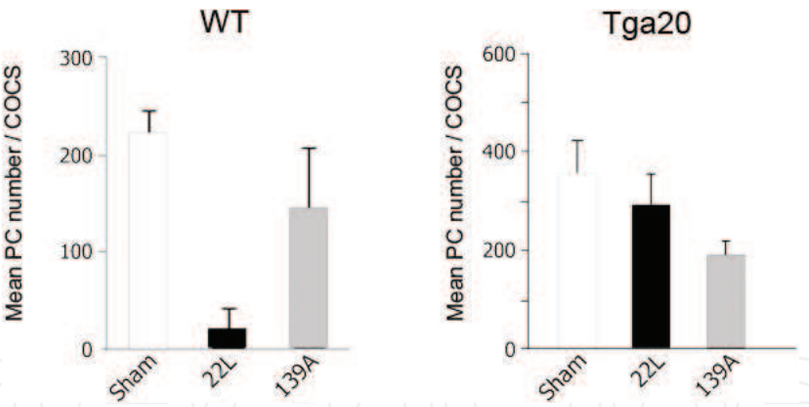

Figure 6.
Mean numbers of CaBP-immunofluorescent PCs in WT and Tga20 COCS noninfected (sham) and infected with 22L and 139A scrapie prions at 30 dpi.

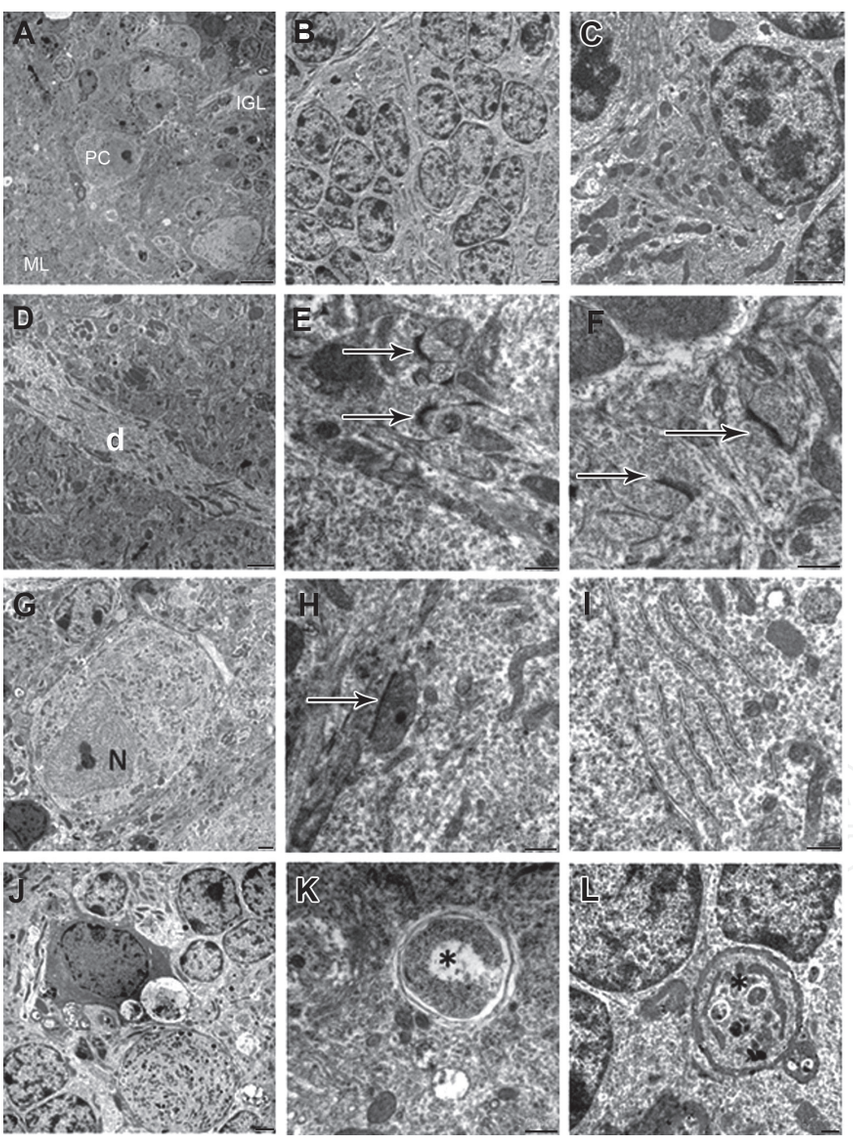

Figure 7.
Ultrastructural features of the C57Bl6/J mouse cerebellar cortex in noninfected COCS after 30 DIV. **A.** *Laminar organization of the cerebellar cortex with PC at the interface between internal granular layer (IGL) and molecular layer (ML).* **B.** *Granule cells in the IGL.* **C.** *IGL neuropil.* **D.** *PC dendrite (d) in the ML neuropil.* **E, F.** *Asymmetrical synapses (arrows) on interneurons dendrites (E) and PC spines (F).* **G.** *PC. N, PC nucleus.* **H.** *A smooth saccule (arrow) typically separates a mitochondrion from the plasma membrane in the PC neuroplasm.* **I.** *Nissl body in the PC neuroplasm.* **J.** *Degenerated cell with electron-dense vacuolated cytoplasm.* **K.** *Autophagic digestion of a mitochondrion (*).* **L.** *Autophagic profiles in a PC axon (*). Scale bars = 10 μm in A, 2 μm in B–D, G, J, 500 nm in E, F, H, I, K, L.*

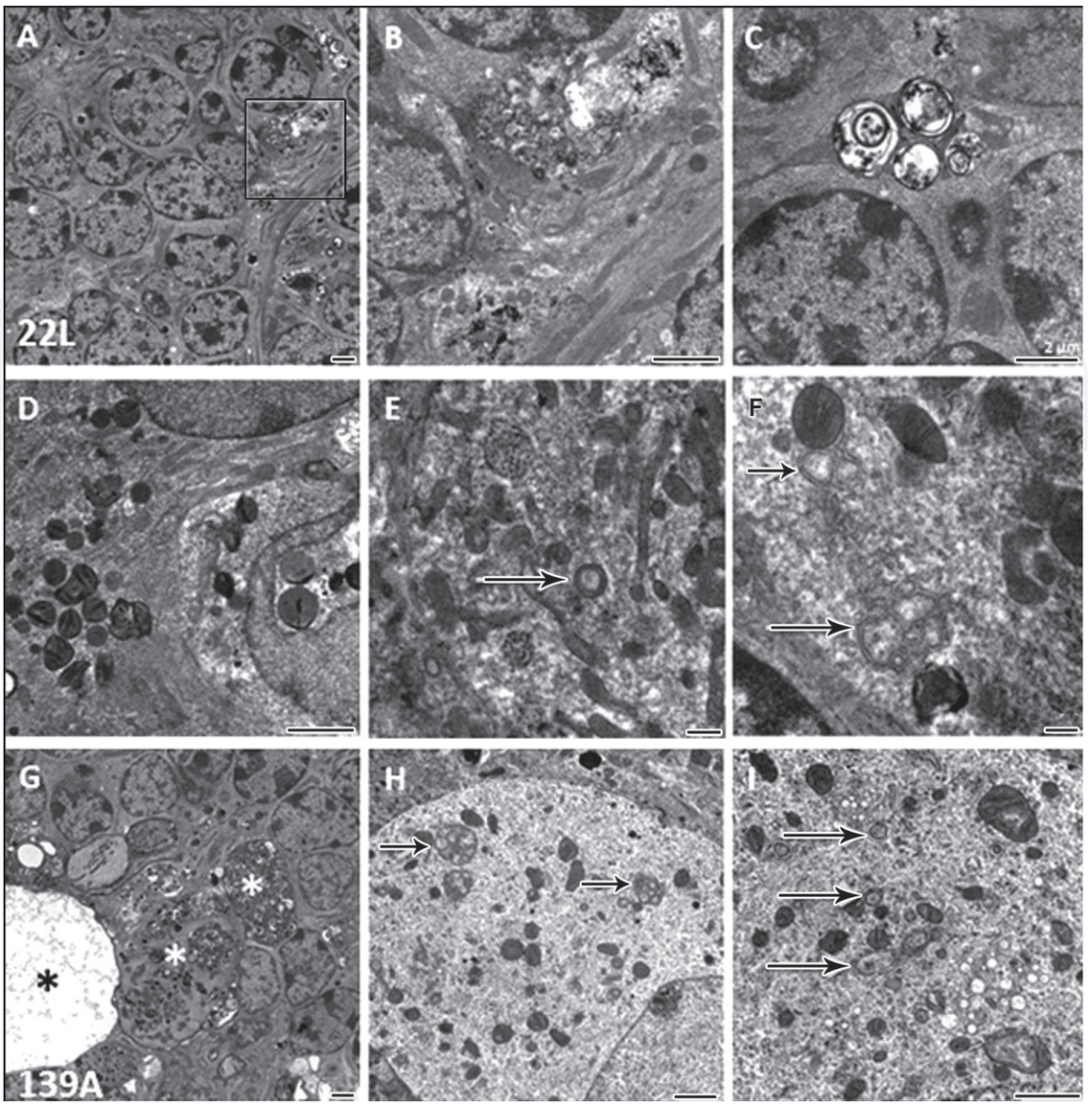

Figure 8.
Cytopathology of the C57Bl6/J mouse cerebellar cortex in COCS infected with 22L (A–F) and 139A (G–L) scrapie prions at 30 dpi. **A.** *IGL.* **B–D.** *Autophagic profiles in the IGL neuropil.* **B.** *Magnification of the inset in A.* **D.** *Electron-dense lysosomes.* **E, F.** *Various stages of ER-derived reticulated organelles (arrows) in the neuroplasm of a PC.* **G.** *Neurodegenerating profiles (*) in the IGL neuropil.* **H, I.** *PC neuroplasm containing different stages of ER-derived reticulated organelles (arrows) and vacuoles. Scale bars = 2 µm in A–D, G–I, 500 nm in E, F.*

alterations were not observed in noninfected slices suggesting that a specific effect of prions links prion-induced ER stress to this morphological ER modification.

2.2 Prion-induced autophagy

Autophagy and apoptosis are activated in many neurodegenerative diseases featured by ubiquitinated misfolded proteins. In neurons, the degradation of abnormal proteins such as α-synuclein in Parkinson's disease, β-amyloid peptide in Alzheimer's disease (AD), or PrP in TSEs occurs by autophagy [14, 132–135]. These cardinal proteins contribute to synaptic dysregulation and altered organelles leading to apoptosis. The neurodegenerating neurons exhibit robust accumulation of cytosolic autophagosomes (see [14] for review, **Figure 10**) suggesting a dysregulation of the autophagic flux resulting from autophagic stress, due to an imbalance between protein synthesis and degradation [136]. Autophagy reduces intraneuronal aggregates and slows down the progression of clinical disease in experimental models of AD [137–139] and prion diseases [140, 141]. Thus, dysregulation of the autophagic

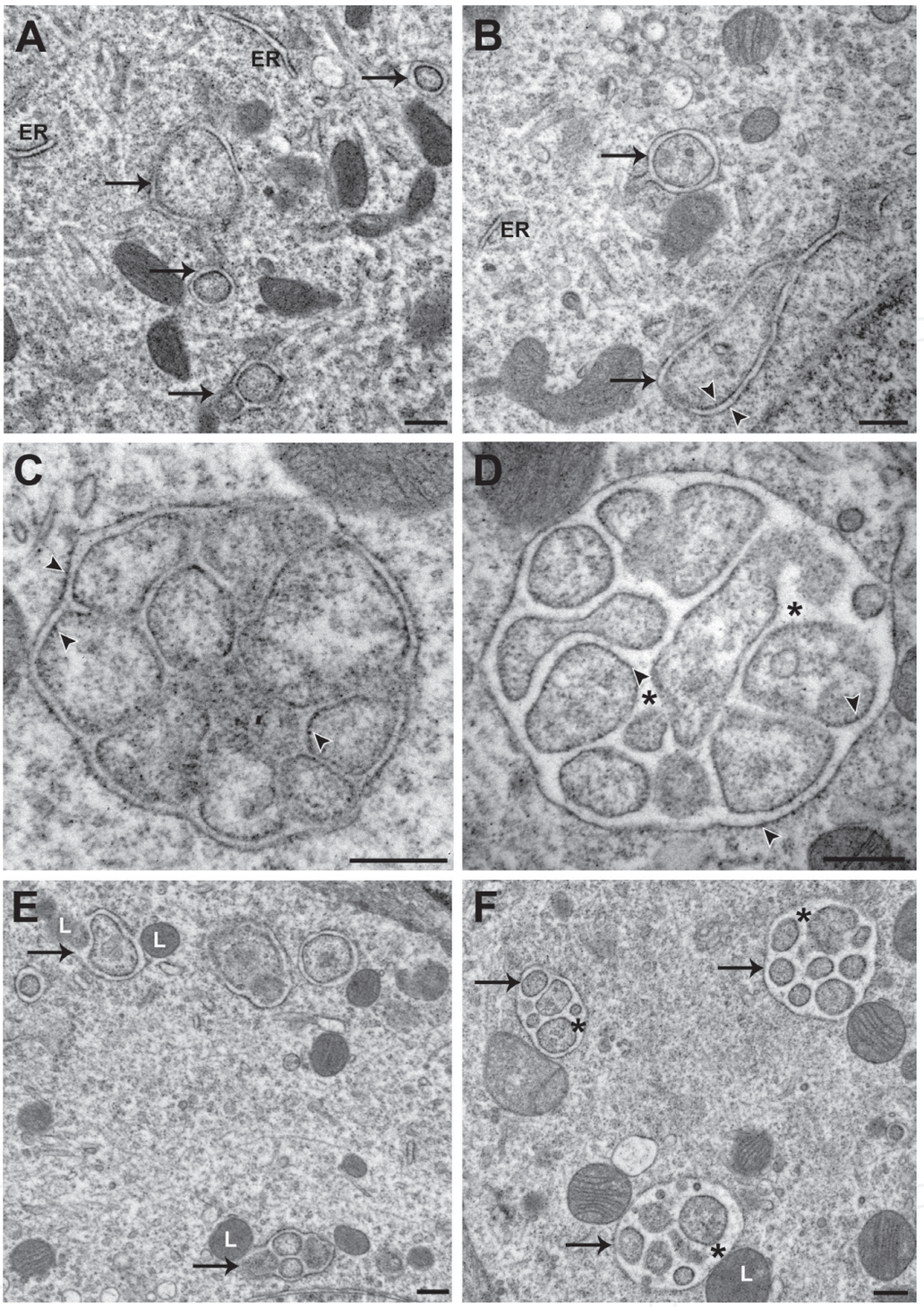

Figure 9.
Cytopathological formation and evolution of ER-derived profiles in PCs of COCS infected with 139A scrapie prions at 30 dpi. **A, B**. *Reticulation and sequestration of neuroplasm by ER saccules forming small double-membrane vesicles (arrows) containing ribosome-like particles (arrowheads in B) on both external and internal faces. ER, endoplasmic reticulum.* **C, D**. *Large compartmented ER-derived organelles which still display membrane-bound ribosomes (arrowheads). C. High magnification of* **Figure 8H**. *D. See the enlargement between membranes (*). **E**. Fusion (arrows) of small ER-derived double-membraned vacuoles with lysosomes (L).* **F**. *Large ER-derived double-membraned vacuoles with enlarged intermembrane space (*) transforming into multivesicular vacuoles (arrows). Scale bars = 500 nm.*

flux impairs the elimination of misfolded proteins and damaged organelles which then accumulate in the cytoplasm and contribute to cell dysfunction and death [142].

Together, spongiform vacuolation of the neuropil, synaptolysis, accompanied by neuronal cell loss and gliosis constitute the classical neuropathological quartet of TSEs. The typical "spongiform vacuoles" are believed to result from autophagy and develop within neuronal elements, myelinated axons, and myelin sheaths

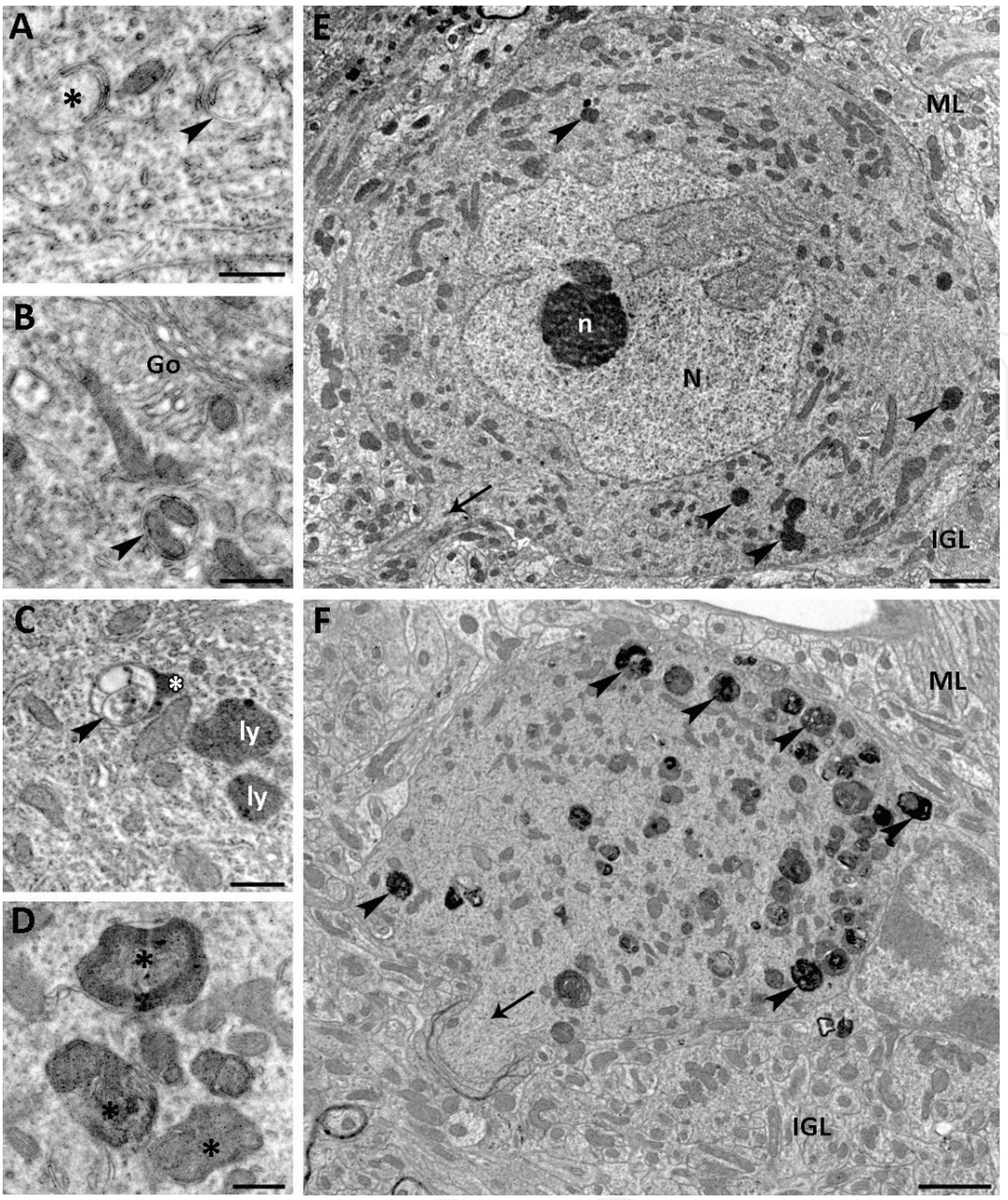

Figure 10.
Autophagy in PCs of 4.5 (A–E) and 12 (F) month-old control $Bax^{+/+}$; $Prnp^{+/+}$ (E) and $Bax^{-/-}$;Ngsk $Prnp^{0/0}$ (A–D, F) mice. Ultrastructural autophagic stages from phagophores to autolysosomes. **A**. *Phagophore (*) and double-membraned autophagosome (arrowhead).* **B**. *Sequestration of two mitochondria in an autophagosome (arrowhead). Go, Golgi dichtyosome.* **C**. *Fusion of an autophagosome (arrowhead) with a lysosome (*). Ly, lysosomes.* **D**. *Autolysosomes (*). A–D. Scale bars = 500 nm.* **E**. *The somato-dendritic cytoplasm of this control $Bax^{+/+}$; $Prnp^{+/+}$ PC contains a few lysosomes and lipofuchsin bodies (arrowheads). N, nucleus; n, nucleolus.* **F**. *Autophagic PC with numerous autophagic organelles (arrowheads) accumulating in the neuroplasm. ML, molecular layer. IGL, internal granular layer. E, F. Arrows show PC axon. Scale bars = 2 μm.*

[143, 144]. Autophagic vacuoles are increased in prion-diseased neurons [64, 65, 145], and the scrapie responsive gene 1 (SRG1) protein is overexpressed and bound to neuronal autophagosomes in the brain of scrapie- and BSE-infected animals and CJD-diseased humans [146, 147]. In addition, LC3-II, a marker of autophagosomes is increased in the cytosol of neurons in scrapie-infected hamsters and CJD- and FFI-diseased patients.

Recent evidence indicated that PrP^c, but not truncated PrP devoid of the N-terminal octapeptide repeat region, exerts a negative control on the induction of autophagy [148]. Thus, the loss or subversion of PrP^c function resulting from prion infection may upregulate autophagy in diseased neurons [16]. While

autophagy-inducing agents increased cellular clearance of PrP^{TSE} [149–151], blocking the fusion of autophagosomes with lysosomes allowed visualization of PrP^{TSE} in the autophagosomes suggesting that degradation of endosomal PrP^{TSE} is by autophagy [134]. However, saturation of the autolysosomal degradation process can release PrP^{TSE} aggregates and degradation enzymes into the neuroplasm contributing to autophagy upregulation and neuronal death [134]. Nevertheless, although autophagy-inducing agents delayed disease onset and PrP^{TSE} accumulation in the CNS of mice [152], survival time was not modified [153]. Along this line, neither autophagy-inducing nor -inhibiting treatments altered the time course or amplitude of prion-induced neuronal death, strongly suggesting that autophagy in protein misfolding diseases is a secondary mechanism in the neurodegenerative process [141, 154].

3. Neuronal death in prion protein-deficient mice

3.1 Impaired autophagy in Zrch-1 prion protein-deficient mice

With the exception of the *Prnp*-knockout models in which ectopic expression of Doppel (Dpl) in the CNS leads to PC death, most other *Prnp*-knockout mouse models do not show gross abnormalities indicating that PrP^c may be dispensable for embryonic development and adulthood. Nevertheless, PrP-deficient mice exhibit an increased predilection for seizures, motor and cognitive disabilities, reduced synaptic inhibition, and long term potentiation in the hippocampus. Also, altered development of the granule cell layer, dysregulation of the cerebellar network and age-dependent spongiform changes with reactive astrogliosis have been observed [155, 156]. In cultures of PrP-deficient hippocampal neurons, autophagy is upregulated in the absence of serum or by hydrogen peroxide-induced oxidative stress [148, 157] suggesting that suppression of the protective effects of PrP^c could impair the autophagic flux in PrP-deficient neurons *in vivo*. Indeed, ultrastructural examination of hippocampus and cerebral cortex of ZH-I $Prnp^{0/0}$ mice revealed an accumulation of autophagosomes containing incompletely digested material increasing from 3 to 12 months of age [158]. In addition, an ultrastructural examination of PCs in the cerebellum of ZH-I $Prnp^{0/0}$ mice revealed significant autophagic accumulation in the somato-dendritic compartment of these neurons from 6 to 14.5 months of age (**Figure 11**). Since autophagic cell death is known to induce neurodegeneration [136, 159, 160], these signs of autophagy blockade could reflect a sustained, progressive autophagic neuronal loss in the CNS of the ZH-I $Prnp^{0/0}$ mice.

3.2 Neuronal loss in Dpl-expressing Ngsk prion protein-deficient mice

Nagasaki (Ngsk) PrP-deficient mice which have a deletion of the entire *Prnp* gene [161–163] develop progressive cerebellar ataxia, which was later discovered to result from the absence of a splice acceptor site in exon 3 of *Prnp* [164]. This leads to the aberrant overexpression of the *Prnd* gene encoding the PrP^c paralogue Dpl [165, 166] that causes selective degeneration of cerebellar PCs. Notably, the reintroduction of *Prnp* in mice overexpressing *Prnd* in the brain rescued the phenotype, suggesting a functional link between the two proteins [167]. Dpl has been shown to have intrinsic neurotoxic properties in cerebellar neurons [168] and has been proposed to interfere with PrP^c and affect cell survival [100]. According to this hypothesis, PrP^c and Dpl bind a common ligand LPrP, where PrP^c binding induces a cell survival signal while Dpl binding activates a death signaling cascade. In PrP^c-deficient *Prnp*-knockout mice that do not express Dpl, the existence of a protein

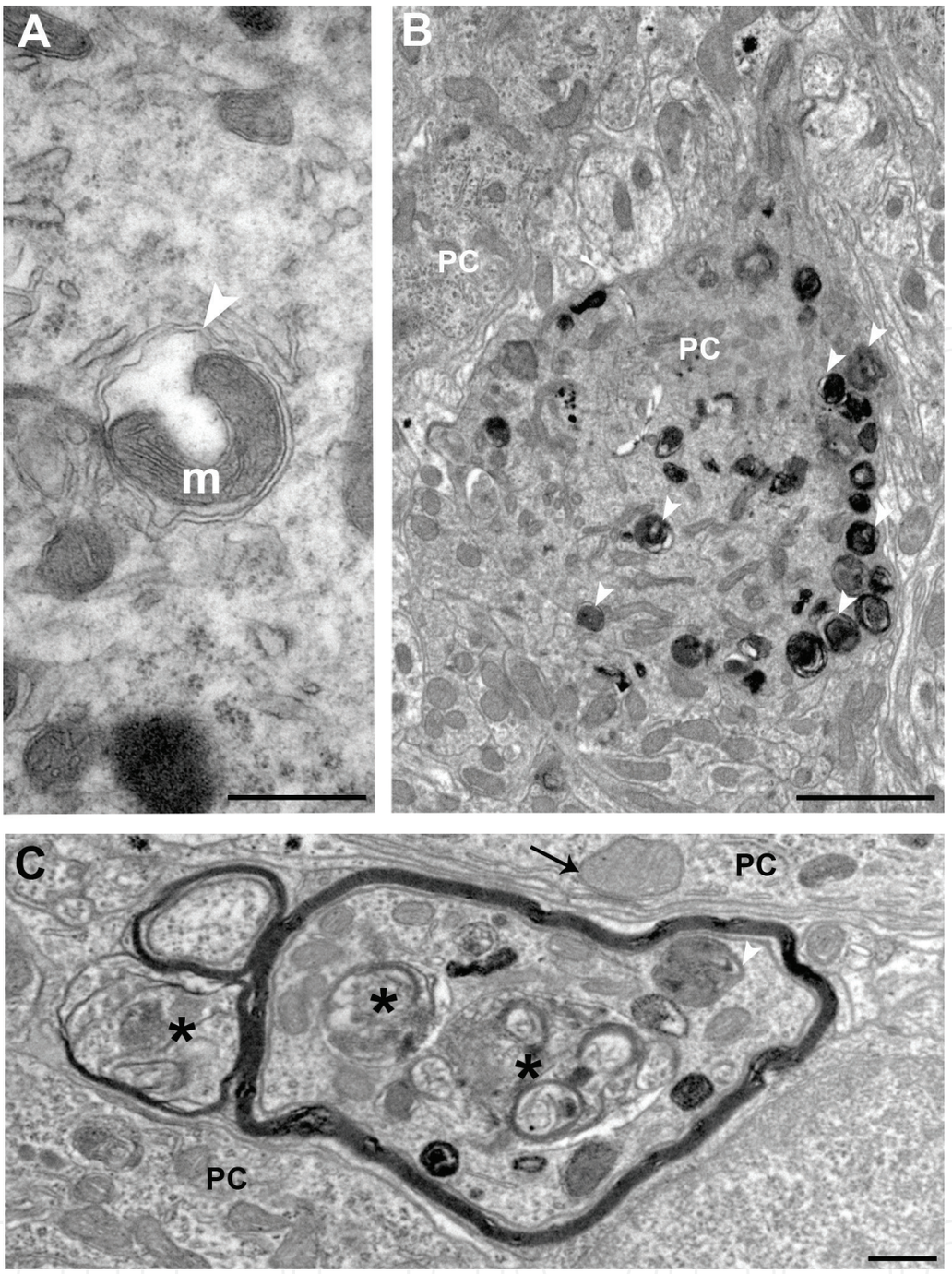

Figure 11.
Autophagy in ZH-I Prnp$^{0/0}$ PCs. **A.** *Mitophagy in the PC neuroplasm of a 4.5 months-old ZH-I Prnp$^{0/0}$ mouse. Arrowhead shows the double membrane of an autophagic vacuole sequestrating a mitochondrion (m). Scale bar = 500 nm.* **B, C.** *12 months-old ZH-I Prnp$^{0/0}$ mice. PC layer. B. Autophagic PC containing numerous autophagosomes and autolysosomes (arrowheads). Scale bar = 2 μm. C. PC layer. Degenerating PC axons containing autophagosomes and lysosomes (*). Scale bar =500 nm.*

π has been proposed to induce a cell survival signal when bound to LPrP [169]. For the moment, LPrP and π remain to be identified, as well as the neuronal death pathways involved in Dpl-induced PC loss.

Because Dpl neurotoxicity depends on PrP^{c}-deficiency in PCs, investigating the underlying neurotoxic mechanism may provide important insight into the neuroprotective function of PrP^{c}. The resistance of the PC population to neurotoxicity increased in the cerebellum of Ngsk mice, which were either deficient for the pro-apoptotic factor Bax [121] or over-express the anti-apoptotic factor Bcl-2 [170]. Although this suggests that an intrinsic apoptotic process is involved in the death of the Ngsk *Prnp*$^{0/0}$ PCs, a significant PC loss still occurred in both

(Bax$^{-/-}$; Ngsk *Prnp*$^{0/0}$) and (HuBcl-2; Ngsk *Prnp*$^{0/0}$) double mutants. Thus, the Ngsk condition, i.e., Dpl neurotoxicity and PrP-deficiency, could activate BAX-independent mechanisms in the Ngsk *Prnp*$^{0/0}$ PCs. These neurons exhibited robust autophagy well before significant neuronal death in the cerebellar cortex of the Ngsk *Prnp*$^{0/0}$ mice [135, 171] suggesting that either "reactive" autophagy is initially induced as a neuroprotective response to Dpl neurotoxicity or impaired autophagy results from PrP-deficiency as in ZH-I *Prnp*$^{0/0}$ mice (see above and [158]). Indeed, the increased expression of the autophagic markers SCRG1, LC3-II, and P62 proteins without any changes in mRNA levels, indicates that the ultimate steps of autophagic degradation are impaired in Ngsk *Prnp*$^{0/0}$ PCs [135]. Probably due to this impairment of autophagic proteolysis, LC3-II-, and Lamp-1-labeled autophagosomes and autolysosomes [172] accumulate in the Ngsk *Prnp*$^{0/0}$ PCs. How apoptosis and autophagy are involved in Ngsk *Prnp*$^{0/0}$ PC death remains to be determined.

To further investigate the role of autophagy in the death of Ngsk *Prnp*$^{0/0}$ PCs, a quantitative analysis of autophagic PCs was performed at the ultrastructural level in the cerebellum of Ngsk *Prnp*$^{0/0}$, *Bax*$^{-/-}$; Ngsk *Prnp*$^{0/0}$, ZCH-I *Prnp*$^{0/0}$ and control *Bax*$^{+/+}$;*Prnp*$^{+/+}$ mice (**Figure 12**). At 4.5 months of age, equivalent amounts of autophagic somato-dendritic compartments and axons of PCs were found in the cerebella of Ngsk *Prnp*$^{0/0}$ and *Bax*$^{-/-}$; Ngsk *Prnp*$^{0/0}$ mutants and were significantly more than those in ZCH-I *Prnp*$^{0/0}$ and control *Bax*$^{+/+}$;Prnp$^{+/+}$ cerebella. Interestingly, the amounts of autophagic axons and somato-dendritic compartments of PCs in the ZCH-I *Prnp*$^{0/0}$ and control *Bax*$^{+/+}$;*Prnp*$^{+/+}$ cerebella were not different. These data suggest that while autophagy induction is already visible in PCs with the Ngsk condition, it is not induced in control *Bax*$^{+/+}$;*Prnp*$^{+/+}$ PCs, nor in the absence of PrP^{c} in the ZCH-I *Prnp*$^{0/0}$ PCs. Thus, autophagy seems to be induced by Dpl neurotoxicity in the Ngsk condition whether BAX is present or not; whereas PrP-deficiency alone has no autophagy-inducing effect at this age (**Figure 13**).

At 6.5–7 months of age, the amount of autophagic somato-dendritic compartments and axons of PC were significantly decreased in *Bax*$^{-/-}$; Ngsk *Prnp*$^{0/0}$ cerebella compared with Ngsk *Prnp*$^{0/0}$ cerebella. Consequently, the amount of autophagic PC profiles in the *Bax*$^{-/-}$; Ngsk *Prnp*$^{0/0}$ and ZH-I *Prnp*$^{0/0}$ cerebella was equivalent, yet more than in the control *Bax*$^{+/+}$;*Prnp*$^{+/+}$ cerebella. Furthermore, autophagic PC somato-dendritic compartments and axons did not change from 4.5 to 6.5–7 months of age in the *Bax*$^{-/-}$; Ngsk *Prnp*$^{0/0}$, whereas many more PCs were autophagic in the 6.5–7 month-old compared to the 4.5 month-old Ngsk *Prnp*$^{0/0}$ cerebella. This increase was also observed in ZH-I *Prnp*$^{0/0}$ cerebella, while no autophagic PCs were found in 6.5–7 month-old control *Bax*$^{+/+}$;*Prnp*$^{+/+}$ cerebella (**Figure 13**).

This suggests that BAX-deficiency modulates autophagy in Ngsk *Prnp*$^{0/0}$ PCs after 4.5 months of age. Autophagy in the ZH-I *Prnp*$^{0/0}$ PCs had increased to the same level as observed in the *Bax*$^{-/-}$;Ngsk *Prnp*$^{0/0}$ cerebella. Thus, the persistent autophagy in the PCs of the *Bax*$^{-/-}$;Ngsk *Prnp*$^{0/0}$ double mutants is likely related to PrP-deficiency. Also, autophagy- and *Bax*-dependent apoptosis are likely to occur in the same PCs that are rescued by *Bax* deletion.

At 12 months of age, the amount of autophagic somato-dendritic compartments and axons of PCs in *Bax*$^{-/-}$;Ngsk *Prnp*$^{0/0}$ cerebella was equivalent to that found in 4.5 month-old cerebella suggesting that autophagy remains stable in this PC population, at a level similar to that maintained in the ZH-I *Prnp*$^{0/0}$, and this likely results from PrP-deficiency. Indeed, many more autophagic PC somato-dendritic compartments and axons were observed in ZH-I *Prnp*$^{0/0}$ cerebella than in the cerebella of 12 month-old control *Bax*$^{+/+}$;*Prnp*$^{+/+}$ mice which did not contain autophagic PCs. However, the autophagic PC somato-dendritic compartments were

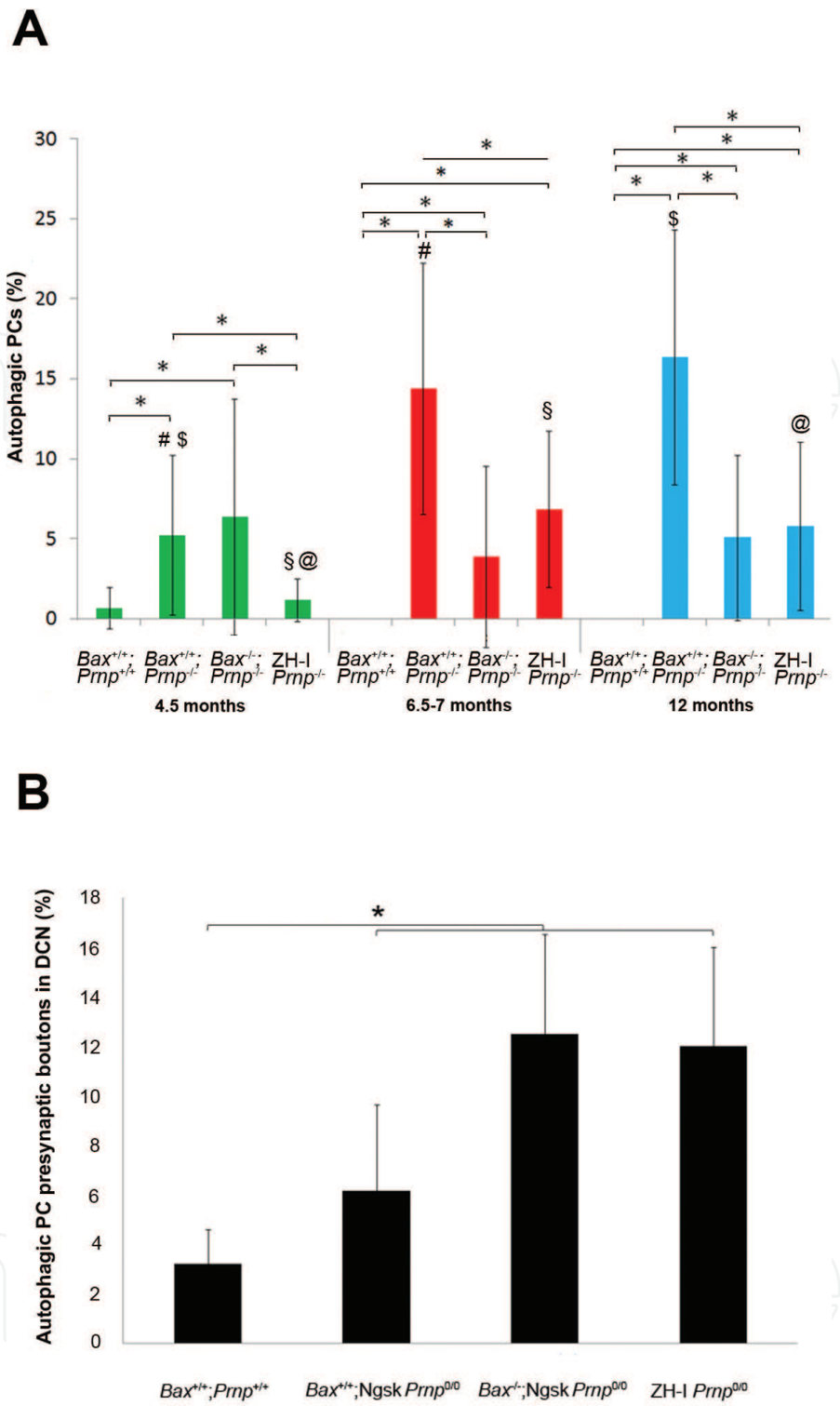

Figure 12.
Quantitative analysis of autophagy in PCs of control Bax$^{+/+}$;Prnp$^{+/+}$ and PrP-deficient Bax$^{+/+}$;Ngsk Prnp$^{o/o}$, Bax$^{-/-}$;Ngsk Prnp$^{o/o}$ and ZH-I Prnp$^{o/o}$ mutant mice. Autophagic somato-dendritic and axonal profiles were counted in 200 PCs in transverse cerebellar sections (50 PCs per hemisphere and hemivermis) from each mouse at 4.5, 6.5–7 and 12 months of age (n = 3 mice/age/genotype). PC soma, primary dendrite and axons were autophagic when containing three or more autophagic profiles (phagophore, autophagosome, autophagolysosome). Data are given as mean values ± standard deviation (SD). Statistical comparisons between ages and genotypes were performed using a two-tailed Student's t test (Statistica). **A.** *Mean percentages of autophagic PC somato-dendritic and axonal compartments. *, #, @, $, §: p < 0.01.* **B.** *Mean percentages of autophagic PC presynaptic boutons making symmetrical synapses on somato-dendritic profiles of deep cerebellar neurons. The PC presynaptic boutons were autophagic when containing at least one autophagic organelle. Autophagic PC presynaptic boutons were counted in 300 presynaptic boutons selected randomly in either left or right fastigial, interposed and dentate nuclei (100 boutons/nucleus) in three 12 month-old mice of each genotype. Statistical comparisons between genotypes were performed using a two-tailed Student's t test (Statistica) and given as mean values ± standard deviation (SD). *, p < 0.01.*

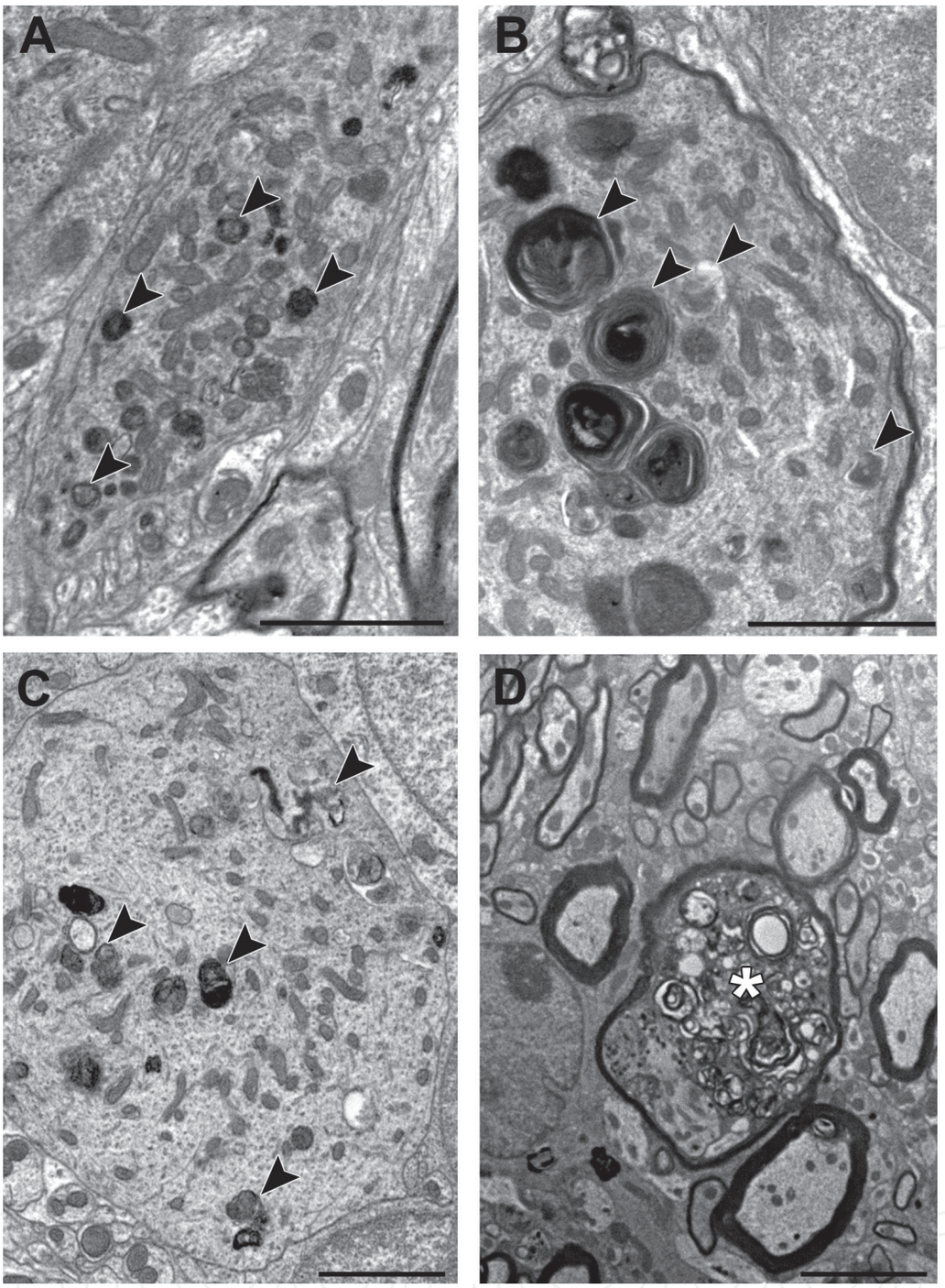

Figure 13.
Autophagy in PCs of 7 (A, B) and 12 (C, D) month-old $Bax^{-/-}$;Ngsk $Prnp^{0/0}$ mice. **A**. *PC-like somato-dendritic profile containing numerous autophagic vacuoles and autolysosomes (arrowheads) in the PC layer.* **B**. *Autolysosomes (arrowheads) in a dystrophic PC-like, myelinated axonal profile in the internal granular layer.* **C**. *Autophagic vacuoles and autolysosomes in a PC-like somato-dendritic profile.* **D**. *Autophagic PC-like myelinated axon (*). Scale bars = 2 μm.*

still more in Ngsk $Prnp^{0/0}$ cerebella (16.36 ± 7.9) compared with $Bax^{-/-}$;Ngsk $Prnp^{0/0}$ (5.08 ± 5) cerebella, and there was a significant increase from 6.5–7 (14.38 ± 7.8) to 12 months of age. The increased amount of autophagic PC axons in $Bax^{-/-}$;Ngsk $Prnp^{0/0}$ cerebella was stable during this same period (3.9 ± 5.6 at 6.5–7 months; 5.08 ± 5.1 at 12 months), suggesting that the initiation of axonal autophagy peaks at 6.5–7 months of age (**Figure 12**) [135, 171, 173–176]. In agreement, an examination of autophagy in the presynaptic terminals of PCs impinging on the somato-dendritic compartments of the deep nuclear neurons in the fastigial, interposed and dentate

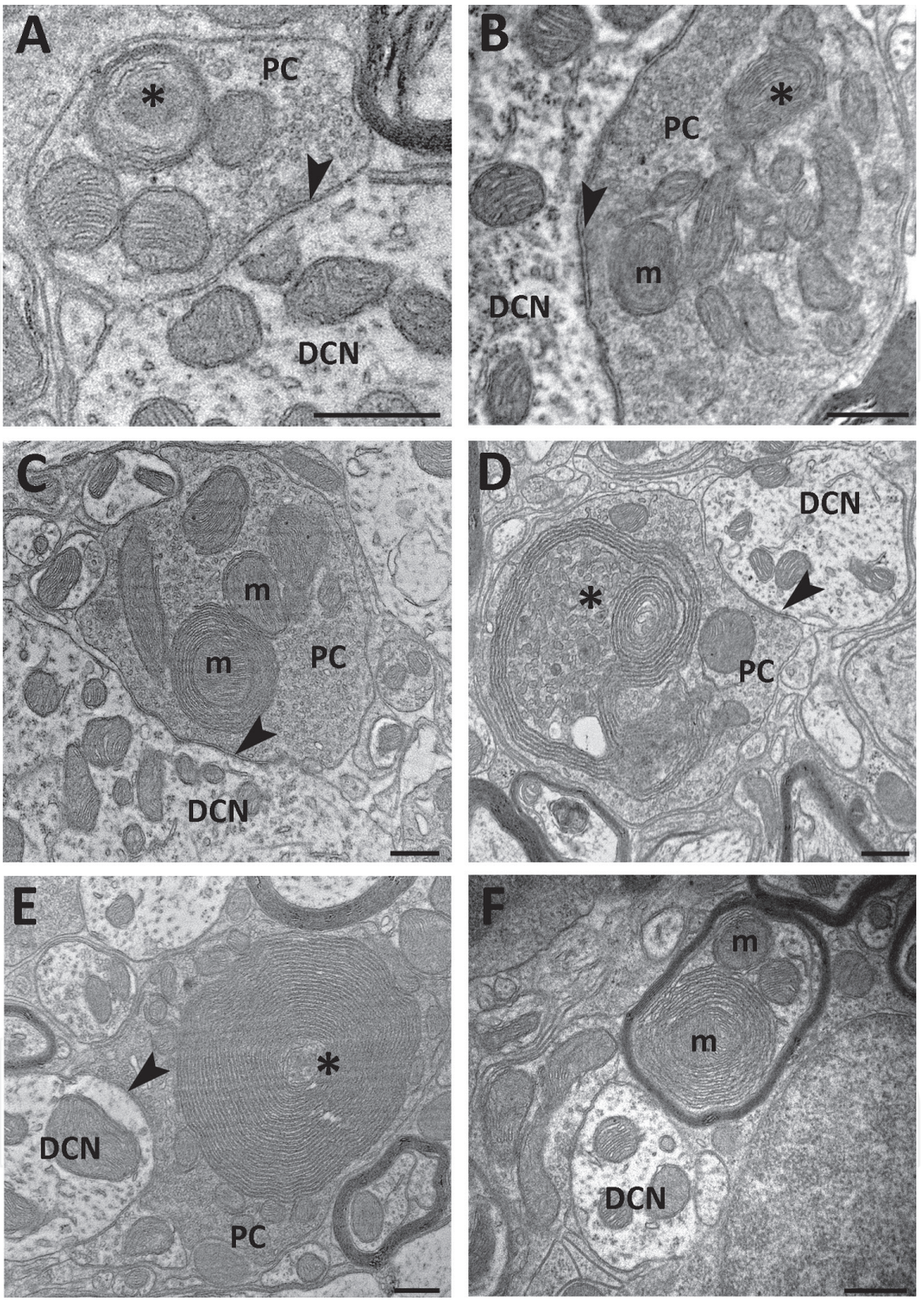

Figure 14.
Autophagy in the deep cerebellar nuclei of 13 month-old Ngsk (A, C–F) and 10 month-old ZH-I (B) $Prnp^{o/o}$ mice. **A–E.** *PC presynaptic boutons establishing symmetrical synapses (arrowheads) with somato-dendritic profiles of deep cerebellar neurons (DCN) and containing different stages of double-membrane wraps sequestrating neuroplasm (* in A, B, D, E) and mitochondria (m in C, F).* **F.** *Myelinated PC-like axon with mitophagic profiles. Scale bars = 500 nm.*

deep cerebellar nuclei, revealed a significantly greater amount of autophagic PC presynaptic boutons in the deep nuclei of all mutants compared to control $Bax^{+/+}$;$Prnp^{+/+}$ mice (**Figure 14**).

The absence of BAX not only protected some PCs from neurotoxicity in the cerebellum of the Ngsk *Prnp*$^{0/0}$ mice [121], but also decreased the number of autophagic neurons suggesting that the PCs rescued by *Bax* deficiency do not display activated autophagy, whereas the autophagic PCs in the *Bax*$^{-/-}$;Ngsk *Prnp*$^{0/0}$ cerebellum are likely to result from PrP-deficiency as in the ZH-I *Prnp*$^{0/0}$ cerebellum. Nevertheless, the persistent loss of Bax$^{-/-}$;Ngsk *Prnp*$^{0/0}$ PCs could result from an increased sensitivity of these PCs to the Ngsk condition compared to ZH-I *Prnp*$^{0/0}$ PCs.

The complex pattern of neuronal death observed in neurodegenerative diseases is believed to involve an extensive interplay between the major cell death pathways [177, 178]. This is likely the case in prion-infected, as well as PrP-deficient neurons such as PCs. We further investigated PC death in Ngsk *Prnp*$^{0/0}$ and ZH-I *Prnp*$^{0/0}$ COCS by measuring PC survival and development using morphometric methods [179] in COCS from these PrP-deficient mice. Similar timing and amplitude of PC growth impairment and death were observed in all PrP-deficient genotypes. Indeed, PC surface, perimeter, and dendritic extension increased between 7 and 21 DIV in the wild-type COCS, while no significant variation of surface and perimeter could be measured in the PrP-deficient mutant COCS during this period (**Figure 15**). Similarly, wild-type and PrP-deficient PCs displayed equivalent maximal dendritic extension after 7 days *ex vivo*, but wild-type PCs continued to increase their maximal dendritic length until 21 DIV, while the dendrites of PrP-deficient PCs did not grow during this period [14, 180]. Thus, PrP-deficient PCs exhibit a similar developmental deficit which seems to be independent of Dpl expression in COCS.

The neurotoxic effects of PrP-deficiency were quantitatively analyzed by counting PCs at 3, 5, 7, 12, and 21 days in COCS from wild-type, Ngsk *Prnp*$^{+/0}$, Ngsk *Prnp*$^{0/0}$, and ZH-I *Prnp*$^{0/0}$. Whereas, wild-type PCs' numbers remained stable during the whole period, severe PC loss (68–69%) had occurred at 7 DIV and slightly increased up to 21 DIV in all PrP-deficient mutant COCS. PC loss displayed similar kinetics and amplitude in Ngsk *Prnp*$^{+/0}$, Ngsk *Prnp*$^{0/0}$, and ZH-I *Prnp*$^{0/0}$ COCS suggesting that despite detectable levels of 15–20 kDa glycosylated form of Dpl in the Ngsk *Prnp*$^{0/0}$ COCS (**Figure 16**), it may be not implicated in PC death in *ex vivo* cultures.

Furthermore, at the ultrastructural level, whereas autophagic organelles were rare in wild-type PCs after 7 and 12 DIV, Ngsk *Prnp*$^{0/0}$ PCs contained numerous autophagosomes and autophagolysosomes at different maturation stages (**Figure 17**). During the period of PC death in the *Prnp*$^{0/0}$ COCS (i.e., 3, 5, and 7 DIV) Western blotting of apoptotic and autophagic markers revealed a 4- to 5-fold increase in markers of autophagosomal formation such as LC3B-II (at 5 DIV), p62, and beclin-1 (at 3 and 5 DIV) in the ZH-I and Ngsk *Prnp*$^{0/0}$ COCS and the lysosomal receptor LAMP-1 in the Ngsk *Prnp*$^{0/0}$ COCS at 7 DIV (**Figure 18**). Increased amounts of activated caspase-3 indicated the apoptosis in protein extracts of COCS from both *Prnp*$^{0/0}$ genotypes as early as 3DIV [14].

This morphometric and quantitative analysis of COCS suggests that PrP-deficiency, rather than Dpl neurotoxicity, is responsible for the neuronal growth deficit and loss *ex vivo*. Indeed, the neurotoxic properties of Dpl did not seem to contribute to Ngsk PC loss in the COCS, whereas Dpl-induced PC loss is detectable in 6-month-old Ngsk *Prnp*$^{0/0}$ mice. A possible explanation for this difference is that COCS are not mature enough to model 6-month-old cerebellar tissue. Nevertheless, in Ngsk *Prnp*$^{0/0}$ and ZH-I *Prnp*$^{0/0}$ COCs, activation of autophagy and apoptosis is contemporaneous with the atrophy and death of PCs during the first week of culture suggesting that PrP-deficiency is solely responsible for neuronal death in this

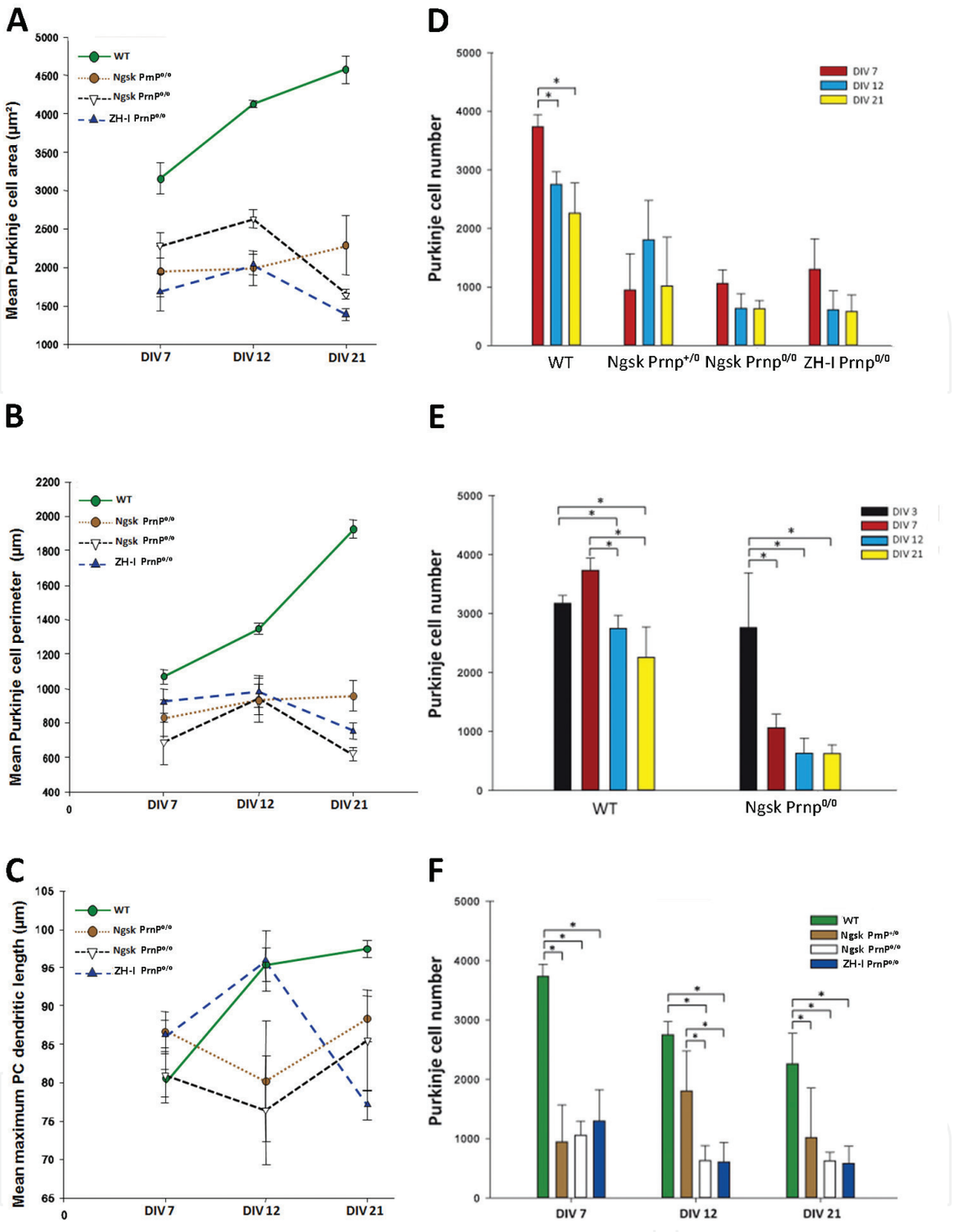

Figure 15.
PC growth deficits and loss in PrP-deficient COCS. **A**, **B**. *PC area (A) and perimeter (B) of WT PCs increased from DIV7 to DIV21, whereas both dimensions in Ngsk Prnp$^{+/0}$, Ngsk Prnp$^{0/0}$ and ZH-I Prnp$^{0/0}$ PCs did not change during the same period. A. At DIV7, WT PC area was larger than area of PrP-deficient PCs.* **C**. *While the longest dendrite of WT PCs had significantly grown from DIV7 to DIV21, the longest dendrite of PrP-deficient PCs displayed similar growth impairment suggesting that in both Ngsk and ZH-I conditions, PrP-deficiency is responsible for PC growth deficits.* **D–F**. *PC loss occurred progressively during the DIV7-DIV21 period in WT COCS (40% at DIV21) while similar loss of PrP-deficient PCs had occurred in the Ngsk Prnp$^{+/0}$, Ngsk Prnp$^{0/0}$ (40%) and ZH-I Prnp$^{0/0}$ (55%) COCS as early as DIV7. E. The Ngsk Prnp$^{0/0}$ COCS had lost many more PCs than the WT COCS over the DIV3-DIV7 period indicating a neurotoxic effect during this period that is attributable to PrP-deficiency since the Ngsk and the ZH-I conditions induced similar neuronal loss at DIV7.*

ex vivo system and that PrP^{c} is neuroprotective for cerebellar PCs. As ZH-I *Prnp*$^{0/0}$ PCs survive *in vivo*, PC death in ZH-I *Prnp*$^{0/0}$ and Ngsk *Prnp*$^{0/0}$ COCS could result from a noxious exacerbation of PrP-deficiency by *ex vivo* conditions.

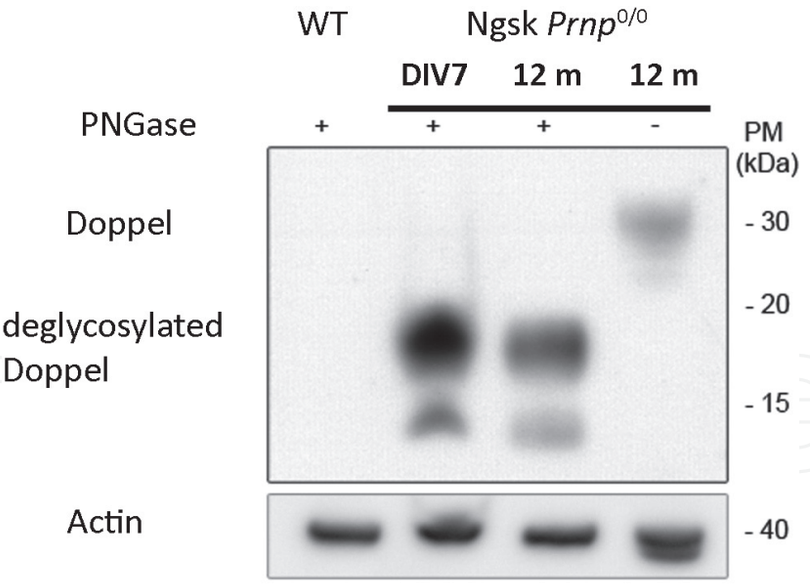

Figure 16.
Western blot of Dpl in Ngsk Prnp$^{0/0}$ DIV7 COCS and 12 month-old mouse cerebellum. Dpl was detected in a Ngsk Prnp$^{0/0}$ COCS at DIV7 and in situ in the cerebellar extract from a 12 month-old Ngsk Prnp$^{0/0}$ mouse but not in the cerebellum of a wild-type (WT) mouse. Dpl migrates at 15–20 kDa after deglycosylation by peptide N-glucosidase (PNGase).

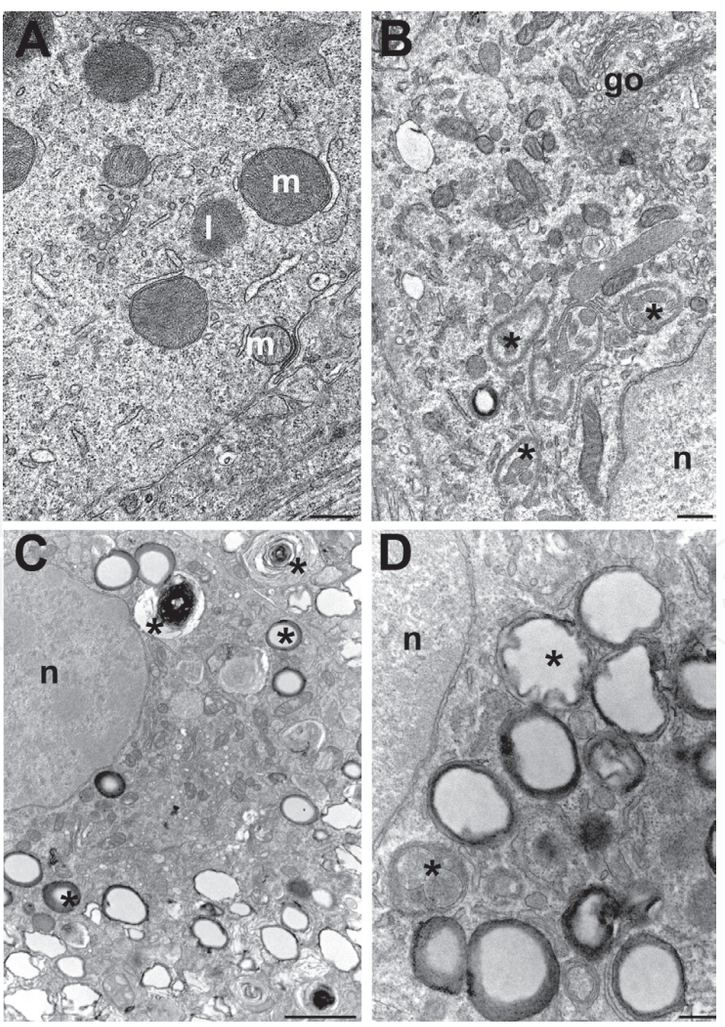

Figure 17.
Autophagy in Ngsk Prnp$^{0/0}$ PCs ex vivo. **A**. *PC cytoplasm in a 12 DIV WT COCS. m, mitochondrion; l, lysosome. Scale bar = 500 nm.* **B–D**. *Autophagic PC cytoplasm in 7 DIV Ngsk Prnp$^{0/0}$ COCSs. Asterisks indicate nascent autophagic vacuoles in B and different maturation stages of autophagolysosomes in C and D. n, nucleus. Scale bar = 2 μm.*

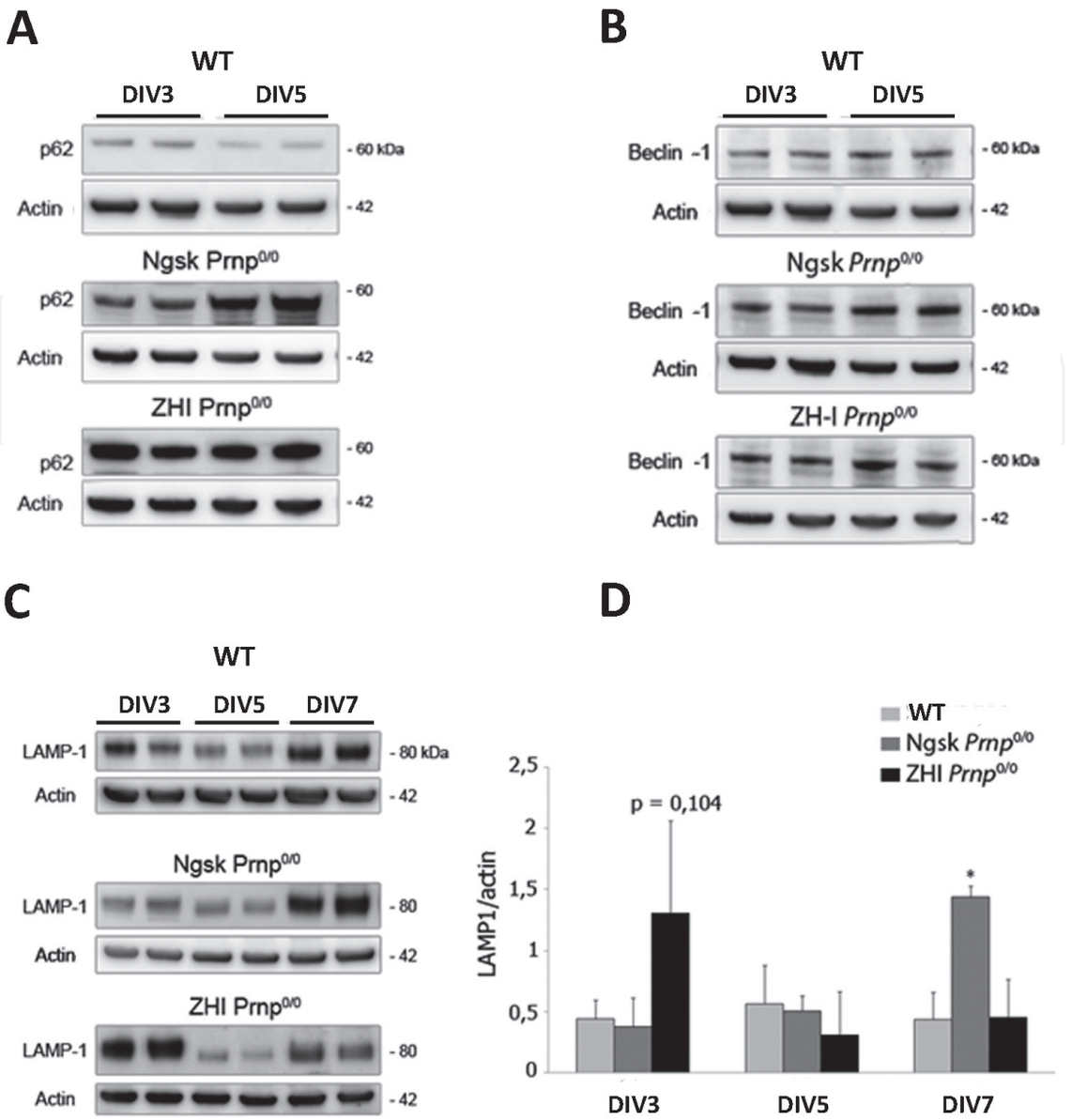

Figure 18.
Western blot of autophagic markers p62, beclin-1 and LAMP-1. **A.** *p62 and* **B.** *Beclin-1. The markers were weakly expressed in WT COCS, but increased in DIV3 and DIV5 COCS from PrP-deficient mice.* **C, D.** *LAMP-1 did not vary in WT and ZH-1 COCS from DIV3 to DIV7, but increased in DIV7 Ngsk Prnp$^{0/0}$ COCS indicating increased lysosomal activity ($p < 0.05$; $n = 3$ mice/genotype and DIV).*

4. Conclusion

Although the contribution of apoptosis to prion-induced death of central neurons including cerebellar ones is strongly supported, our studies of scrapie-infected PCs show that although caspase-3 is activated, the pro-apoptotic BAX/BCL-2-dependent mitochondrial pathway is not involved in the prion-induced death of these neurons. This is also the case for BSE-induced death of hippocampal and thalamic neurons [119], suggesting that prions exert neurotoxicity through BAX-independent activation of caspase-3. Ultrastructural evidence of ER stress and robust autophagy in the scrapie-infected cerebellar neurons both *in vivo* and *ex vivo* implicate them in these BAX-independent neurotoxic mechanisms. Furthermore, the autophagic blockade resulting from prion protein-deficiency in ZH-I and Ngsk *Prnp*$^{0/0}$ mice may contribute to neuronal death in infectious prion-diseased cerebellar neurons. In Ngsk *Prnp*$^{0/0}$ cerebellar neurons, Dpl neurotoxicity and PrP-deficiency contribute to neuronal death probably through an interplay between autophagic blockade and BAX-dependent apoptosis.

DOI: http://dx.doi.org/10.5772/intechopen.80701

Author details

Audrey Ragagnin[1], Qili Wang[1], Aurélie Guillemain[1], Siaka Dole[1], Anne-Sophie Wilding[1], Valérie Demais[1,2], Cathy Royer[1,2], Anne-Marie Haeberlé[1], Nicolas Vitale[1], Stéphane Gasman[1], Nancy Grant[1] and Yannick Bailly[1]*

1 Intracellular Membrane Trafficking in the Nervous and Neuroendocrine System, INCI, CNRS UPR3212, University of Strasbourg, Strasbourg, France

2 In Vitro Imaging Platform, CNRS UPS 3156, University of Strasbourg, Strasbourg, France

*Address all correspondence to: byan@inci-cnrs.unistra.fr

References

[1] Collinge J. Prion diseases of human and animals: Their causes and molecular basis. Annual Review of Neuroscience. 2001;**24**:519-550

[2] Morales R. Prion strains in mammals: Different conformations leading to disease. PLoS Pathogens. 2017;**13**:e1006323. DOI: 10.1371/journal.ppat.1006323

[3] Ironside JW, Ritchie DL. Head MW prion diseases. Handbook of Clinical Neurology. 2018;**145**:393-403. DOI: 10.1016/B978-0-12-802395-2.00028-6

[4] Babelhadj B, Di Bari MA, Pirisinu L, Chiappini B, Gaouar SBS, Riccardi G, et al. Prion disease in dromedary camels, Algeria. Emerging Infectious Diseases. Jun 2018;**24**(6):1029-1036. DOI: 10.3201/eid2406.172007

[5] Prusiner S. Novel proteinaceous infection particles cause scrapie. Science. 1982;**216**:136-144

[6] Brandner S, Raeber A, Sailer A, Blättler T, Fischer M, Weissmann C, et al. Normal host prion protein (PrPC) is required for scrapie spread within the central nervous system. Proceedings of the National Academy of Sciences of the United States of America. 1996;**93**:13148-13151

[7] Aguzzi A, Polymenidou M. Mammalian prion biology: One century of evolving concepts. Cell. 2004;**116**:313-327

[8] Büeler HR, Fischer M, Lang Y, Bluethmann H, Lipp HP, DeArmond SJ, et al. Normal development and behaviour of mice lacking the neuronal cell-surface PrP protein. Nature. 1992;**356**:577-582. DOI.org/10.1038/356577a0

[9] Manson JC, Clarke AR, Hooper ML, Aitchison L, McConnell I, Hope J. 129/Ola mice carrying a null mutation in PrP that abolishes mRNA production are developmentally normal. Molecular Neurobiology. 1994;**8**:121-127

[10] Nuvolone M, Hermann M, Scorce S, Russo G, Tiberi C, Schwarz P, et al. Strictly co-isogenic C57BL/6J-*Prnp*$^{-/-}$ mice: A rigorous resource for prion science. The Journal of Experimental Medicine. 2016;**213**:313-327

[11] Büeler H, Aguzzi A, Sailer A, Greiner RA, Autenried P, Aguet M, et al. Mice devoid of PrP are resistant to scrapie. Cell. 1993;**73**:1339-1347

[12] Mallucci GR, Ratte S, Asante EA, Linehan J, Gowland I, Jefferys JGR, et al. Post-natal knockout of prion protein alters hippocampal CA1 properties but does not result in neurodegeneration. The EMBO Journal. 2002;**21**:202-210

[13] Wulf MA, Senatore A, Aguzzi A. The biological function of the cellular prion protein: An update. BMC Biology. 2017;**15**:34. DOI: 10.1186/s12915-017-0375-5

[14] Ragagnin A, Guillemain A, Grant NJ, Bailly Y. Neuronal autophagy and prion proteins. In: Bailly YJR, editor. Autophagy—A Double-Edged Sword—Cell Survival or Death? Rijeka, Croatia: InTech Publisher; 2013. pp. 377-419

[15] Legname G. Elucidating the function of the prion protein. PLoS Pathogens. Aug 31, 2017;**13**(8):e1006458. DOI: 10.1371/journal.ppat.1006458

[16] Saa P, Harris D, Cervenakova L. Mechanisms of prion-induced neurodegeneration. Expert Reviews in Molecular Medicine. Apr 8, 2016;**18**:e5. DOI: 10.1017/erm2016.8

[17] Stahl N, Borchelt DR, Hsiao K, Prusiner SB. Scrapie prion protein

contain a phosphatidylinositol glycolipid. Cell. 1987;**51**:229-240

[18] Lainé J, Marc M, Sy M, Axelrad H. Cellular and subcellular morphological localization of normal prion protein in rodent cerebellum. The European Journal of Neuroscience. 2001;**14**:47-56

[19] Bailly Y, Haeberlé AM, Blanquet-Grossard F, Chasserot-Golaz S, Grant N, Schulze T, et al. Prion protein (PrP^c) immunocytochemistry and expression of the green fluorescent protein reporter gene under the control of bovine PrP gene promoter in the mouse brain. The Journal of Comparative Neurology. 2004;**473**:244-269

[20] Jacobson K, Dietrich C. Looking at lipid rafts? Trends in Cell Biology. 1999;**9**:87-91

[21] Mouillet-Richard S, Ermonval M, Chebassier C, Laplanche JL, Lehmann S, Launay JM, et al. Signal transduction through prion protein. Science. 2000;**289**:1925-1928. Epub Sep 16, 2000. DOI: 10.1126/science.289.5486.1925

[22] Linden R, Martins VR, Prado MA, Cammarota M, Izquierdo I, Brentani RR. Physiology of the prion protein. Physiological Reviews. 2008;**88**:673-728

[23] Bendheim PE, Brown HR, Rudelli RD, Scala LJ, Goller NL, Wen GY, et al. Nearly ubiquitous tissue distribution of the scrapie agent precursor protein. Neurology. 1992;**42**:149

[24] Haeberlé AM, Ribaut-Barassin C, Bombarde G, Mariani J, Hunsmann G, Grassi J, et al. Synaptic prion protein immuno-reactivity in the rodent cerebellum. Microscopy Research and Technique. 2000;**50**:66-75

[25] Salès N, Rodolfo K, Hässig R, Faucheux B, Di Giamberardino L, Moya KL. Cellular prion protein localization in rodent and primate brain. The European Journal of Neuroscience. 1998;**10**:2464-2471

[26] Salès N, Hässig R, Rodolfo K, Di Giamberardino L, Traiffort E, Ruat M, et al. Developmental expression of the cellular prion protein in elongating axons. The European Journal of Neuroscience. 2002;**15**:1163-1177

[27] Fournier JG, Escaig-Haye F, Billette de Villemeur T, Robain O. Ultrastructural localization of cellular prion protein (PrPc)in synaptic boutons of normal hamster hippocampus. Comptes Rendus de l'Académie des Sciences, Paris. 1995;**318**:339-344

[28] Herms J, Tings T, Gall S, Madlung A, Giese A, Siebert H, et al. Evidence of presynaptic location and function of the prion protein. The Journal of Neuroscience. 1999;**19**:8866-8875

[29] Mironov A, Latawiec D, Wille H, Bouzamondo-Bernstein E, Legname G, Williamson RA, et al. Cytosolic prion protein in neurons. The Journal of Neuroscience. 2003;**23**:183-193

[30] Borchelt DR, Koliatsos VE, Guarnieri M, Pardo CA, Sisodia SS, Price DL. Rapid anterograde axonal transport of the cellular prion glycoprotein in the peripheral and central nervous systems. The Journal of Biological Chemistry. 1994;**269**:14711-14714

[31] Moya K, Hässig R, Créminon C, Laffont I, Di Giamberardino L. Enhanced detection and retrograde axonal transport of PrPc in peripheral nerve. Journal of Neurochemistry. 2003;**88**:155-160

[32] Jeffrey M, Halliday WG, Bell J, Johnston AR, McLeod NK, Ingham C, et al. Synapse loss associated with abnormal PrP precedes neuronal degeneration

in the scrapie-infected murine hippocampus. Neuropathology and Applied Neurobiology. 2000;**26**:41-54

[33] Siskova Z, Reynolds RA, O'Connor V, Perry VH. Brain region specific presynaptic and postsynaptic degeneration are early components of neuropathology in prion diseases. PLoS One. 2013;**8**(1):e55004. DOI: 110.1371/journal.pone.0055004

[34] Senatore A, Colleoni S, Verderio C, Restelli E, Morini R, Condliffe SB, et al. Mutant PrP suppresses glutamatergic neurotransmission in cerebellar granule neurons by impairing membrane delivery of VGCC α2δ-1 subunit. Neuron. 2012;**74**:300-313. DOI: 10.1016/j.neuron.2012.02.027

[35] Khosravani H, Zhang Y, Tsutsui S, Hameed S, Altier C, Hamid J, et al. Prion protein attenuates excitotoxicity by inhibiting NMDA receptors. The Journal of Cell Biology. 2008;**181**:551-565. DOI: 10.1083/jcb.200711002

[36] Mercer RCC, Ma L, Watts JC, Strome R, Wohlgemuth S, Yang J, et al. The prion protein modulates A-typeK+ currents mediated by Kv4.2 complexes through dipeptidyl aminopeptidase-like protein 6. The Journal of Biological Chemistry. 2013;**288**:37241-37255

[37] Stys PK, You H, Zamponi GW. Copper-dependent regulation of NMDA receptors by cellular prion protein: Implications for neurodegenerative disorders. The Journal of Physiology. 2012;**590**:1357-1368. DOI: 10.1113/jphysiol.2011.225276

[38] Gasperini L, Meneghette E, Pastore B, Benetti F, Legname G. Prion protein and copper cooperatively protect neurons by modulating NMDA receptors through S-nitrosylation. Antioxidants & Redox Signaling. 2015;**22**:772-784

[39] Muller WE, Ushijima H, Schroder HC, Forrest JM, Schatton WF, Rytik PG, et al. Cytoprotective effect of NMDA receptor antagonists on prion protein (PrioSc)-induced toxicity in rat cortical cell cultures. European Journal of Pharmacology. 1993;**246**:261-267

[40] Resenberger UK, Harmeier A, Woerner AC, Goodman JL, Muller V, Krishnan R, et al. The cellular prion protein mediates neurotoxic signalling of eIF2α-sheet-rich conformers independent of prion replication. The EMBO Journal. 2011;**30**:2057-2070. DOI: 10.1038/emboj.2011.86

[41] Carulla P, Llorens F, Matamoros-Angles A, Aguilar-Calvo P, Espinosa JC, Gavín R, et al. Involvement of PrP(C) in kainate-induced excitotoxicity in several mouse strains. Scientific Reports. 2015;**5**:11971. DOI: 10.1038/srep11971

[42] Kleene R, Loers G, Langer J, Frobert Y, Buck F, Schachner M. Prion protein regulates glutamate-dependent lactate transport of astrocytes. The Journal of Neuroscience. 2007;**27**:12331-12340

[43] Watt NT, Taylor DR, Kerrigan TL, Griffiths HH, Rushworth JV, Whitehouse IJ, et al. Prion protein facilitates uptake of zinc into neuronal cells. Nature Communications. 2012;**3**:1134

[44] Beraldo FH, Arantes CP, Santos TG, Machado CF, Roffe M, Hajj GN, et al. Metabotropic glutamate receptors transducer signals for neurite outgrowth after binding of the prion protein to laminin γ1 chain. The FASEB Journal. 2011;**25**:265-279

[45] Um JW, Kaufman AC, Kostylev M, Heiss JK, Stagi M, Takahashi H, et al. Metabotropic glutamate receptor 5 is a coreceptor for Alzheimer eIF2α oligomer bound to cellular prion protein. Neuron. 2013;**79**:887-902

[46] Lauren J, Gimbel DA, Nygaard HB, Gilbert JW, Strittmatter SM. Cellular prion protein mediates impairment of synaptic plasticity by amyloid-β oligomers. Nature. 2009;**457**:1128-1132

[47] Um JW, Nygaard HB, Heiss JK, Kostylev MA, Stagi M, Wortmeyer A, et al. Alzheimer amyloid-β oligomer bound to postsynaptic prion protein activates Fyn to impair neurons. Nature Neuroscience. 2012;**15**:1227-1235

[48] Winklhofer KF, Tatzelt J, Haass C. The two faces of protein misfolding: Gain- and loss-of-function in neurodegenerative diseases. The EMBO Journal. 2008;**27**:336-349

[49] Harris DA, True HL. New insights into prion structure and toxicity. Neuron. 2006;**50**:353-357

[50] Moreno JA, Radford H, Peretti D, Steinert JR, Verity N, Martin MG, et al. Sustained translational repression by eIF2α-P mediates prion neurodegeneration Nature. 2012;**485**:507-511. DOI: 10.1038/nature11058. Erratum in: Nature. 2014;**511**:370

[51] McKinnon C, Goold R, Andre R, Devoy A, Ortega Z, Moonga J, et al. Prion-mediated neurodegeneration is associated with early impairment of the ubiquitin-proteasome system. Acta Neuropathologica. 2016;**131**:411-425. DOI: 10.1007/s00401-015-1508-y

[52] Hegde RS, Tremblay P, Groth D, DeArmond SJ, Prusiner SB, Lingappa VR. Transmissible and genetic prion diseases share a common pathway of neurodegeneration. Nature. 1999;**402**:822-826

[53] Moreno JA, Halliday M, Molloy C, Radford H, Verity N, Axten JM, et al. Oral treatment targeting the unfolded protein response prevents neurodegeneration and clinical disease in prion-infected mice. Science Translational Medicine. Oct 9, 2013;**5**(206):206ra138. DOI: 10.1126/scitranslmed.3006767

[54] Telling GC. The importance of prions. PLoS Pathogens. 2013;**9**:e1003090. DOI: 10.1371/journal.ppat.1003090

[55] Piétri M, Dakowski C, Hannaoui S, Alleaume-Buteaux A, Hernandez-Rapp J, Ragagnin A, et al. PDK1 decreases TACE-mediated α-secretase activity and promotes disease progression in prion and Alzheimer's diseases. Nature Medicine. 2013;**19**:1124-1131

[56] Alleaume-Buteaux A, Nicot S, Piétri M, Baudry A, Dakowski C, Tixador P, et al. Double-edge sword of sustained ROCK activation in prion diseases through neuritogenesis defects and prion accumulation. PLoS Pathogens. 2015;**11**:e1005073

[57] Ezpeleta J, Boudet-Devaud F, Piétri M, Baudry A, Baudouin V, Alleaume-Buteaux A, et al. Protective role of cellular prion protein against TNFα-mediated inflammation through TACE α-secretase. Scientific Reports. 2017;**7**:7671. DOI: 10.1038/s41598-017-08110-x

[58] Hilton KJ, Cunningham C, Reynolds RA, Perry VH. Early hippocampal synaptic loss precedes neuronal loss and associates with early behavioural deficits in three distinct strains of prion disease. PLoS One. 2013;**8**:e68062. DOI: 10.1371/journal.pone.0068062

[59] Ragagnin A, Ezpeleta J, Guillemain A, Boudet-Devaud F, Haeberlé A-M, Demais V, et al. Cerebellar compartmentation of prion pathogenesis. Brain Pathology. 2017;**28**:240-263. DOI: 10.1111/bpa.12503

[60] Kristiansen M, Deriziotis P, Dimcheff DE, Jackson GS, Ovaa H, Naumann H, et al. Disease-associated prion protein oligomers inhibit the 26S proteasome. Molecular Cell. 2007;**26**:175-188

[61] Pietri M, Caprini A, Mouillet-Richard S, Pradines E, Ermonval M, Grassi J, et al. Overstimulation of PrPC signaling pathways by prion peptide 106-126 causes oxidative injury of bioaminergic neuronal cells. The Journal of Biological Chemistry. 2006;**281**:28470-28479

[62] Heiseke A, Aguib Y, Schatzl HM. Autophagy, prion infection and their mutual interactions. Current Issues in Molecular Biology. 2010;**12**:87-98

[63] Sikorska B. Mechanisms of neuronal death in transmissible spongiform encephalopathies. Folia Neuropathologica. 2004;**42**(Suppl B): 89-95

[64] Liberski PP, Brown DR, Sikorska B, Caughey B, Brown P. Cell death and autophagy in prion diseases (transmissible spongiform encephalopathies). Folia Neuropathologica. 2008;**46**:1-25

[65] Sikorska B, Liberski PP, Giraud P, Kopp N, Brown P. Autophagy is a part of ultrastructural synaptic pathology in Creutzfeldt-Jakob disease: A brain biopsy study. The International Journal of Biochemistry & Cell Biology. 2004;**36**:2563-2573

[66] Bruce ME, McBride PA, Jeffrey M, Scott JR. PrP in pathology and pathogenesis in scrapie-infected mice. Molecular Neurobiology. 1994;**8**:105-112

[67] Jeffrey M, McGovern G, Sisó S, González L. Cellular and sub-cellular pathology of animal prion diseases: Relationship between morphological changes, accumulation of abnormal prion protein and clinical disease. Acta Neuropathologica. 2011;**121**:113-134

[68] DeArmond SJ, Sánchez H, Yehiely F, Qiu Y, Ninchak-Casey A, Daggett V, et al. Selective neuronal targeting in prion disease. Neuron. 1997;**19**:1337-1348

[69] Lawson VA, Collins SJ, Masters CL, Hill AF. Prion protein glycosylation. Journal of Neurochemistry. 2005;**93**:793-801

[70] Beekes M, McBride PA. The spread of prions through the body in naturally acquired transmissible spongiform encephalopathies. The FEBS Journal. 2007;**274**:588-605

[71] Fraser H, Dickinson AG. The sequential development of the brain lesion of scrapie in three strains of mice. Journal of Comparative Pathology. 1968;**78**:301-311

[72] Guentchev M, Wanschitz J, Voigtländer T, Flicker H, Budka H. Selective neuronal vulnerability in human prion diseases. Fatal familial insomnia differs from other types of prion diseases. American Journal of Pathology. 1999;**155**:1453-1457

[73] Somerville RA. How independent are TSE agents from their hosts? Prion. 2013;**7**:272-275. DOI: 10.4161/pri.25420

[74] Fraser H. Neuropathology of Scrapie: The Precision of Lesion and their Diversity. Slow Transmissible Diseases of the Nervous System. NY: Academic Press; 1979. pp. 387-406

[75] Kim YS, Carp RI, Callahan SM, Natelli M, Wisniewski HM. Vacuolization, incubation period and survival time analyses in three mouse genotypes injected stereotactically in three brain regions

with the 22L scrapie strain. Journal of Neuropathology and Experimental Neurology. 1990;**49**:106-113

[76] Lucassen PJ, Williams A, Chung WCJ, Fraser H. Detection of apoptosis in murine scrapie. Neuroscience Letters. 1995;**198**:185-188

[77] Williams A, Lucassen P, Ritchie D, Bruce M. PrP deposition, microglial activation and neuronal apoptosis in murine scrapie. Experimental Neurology. 1997;**144**:433-438

[78] Fraser J, Halliday W, Brown D, Belichenko P, Jeffrey M. Mechanisms of scrapie-induced neuronal cell death. In: Court L, Dodet B, editors. Transmissible Subacute Spongiform Encephalopathies: Prion Diseases. Paris: Elsevier; 1996. pp. 107-112

[79] Haw JJ, Gray F, Baudrimont M, Escourolle R. Cerebellar changes in 50 cases of Creutzfeldt-Jakob disease with emphasis on granule cell atrophy variant. Acta Neuropathologica. 1981;**7**:196-198

[80] Berciano J, Berciano MT, Polo JM, Figols J, Ciudad J, Lafarga M. Creutzfeldt-Jakob disease with severe involvement of cerebral white matter and cerebellum. Wirschows Archiv. 1990;**417**:533-538

[81] Budka H, Aguzzi A, Brown P, Brucher JM, Bugiani O, Gullotta F, et al. Neuropathological diagnostic criteria for Creutzfeldt-Jakob disease (CJD) and other human spongiform encephalopathies (prion disease). Brain Pathology. 1995;**5**:459-466

[82] Schulz-Schaeffer WJ, Giese A, Windl O, Kretzschmar HA. Polymorphism at codon 129 of the prion protein gene determines cerebellar pathology in Creutzfeldt-Jakob disease. Clinical Neuropathology. 1996;**15**:353-357

[83] Yang Q, Hashizume Y, Yoshida M, Wang Y. Neuropathological study of cerebellar degeneration in prion disease. Neuropathology. 1999;**19**:33-39

[84] Armstrong R, Ironside J, Lantos P, Cairns N. A quantitative study of the pathological changes in the cerebellum in 15 cases of variant Creutzfeldt-Jakob disease (vCJD). Neuropathology and Applied Neurobiology. 2009;**35**:36-45. DOI: 10.1111/j.1365-2990.2008.00979.x

[85] Faucheux B, Morain E, Diouron V, Brandel J, Salomon D, Sazdovitch V, et al. Quantification of surviving cerebellar granule neurons and abnormal prion protein (PrPSc) deposition in sporadic Creutzfeldt-Jakob disease supports a pathogenic role for small PrPSc deposits common to the various molecular subtypes. Neuropathology and Applied Neurobiology. 2011;**37**:500-512. DOI: 10.1111/j.1365-2990.2011.01179.x

[86] Parchi P, Strammiello R, Giese A, Kretzschmar H. Phenotypic variability of sporadic human prion disease and its molecular basis: Past, present and future. Acta Neuropathologica. 2011;**121**:91-112. DOI: 10.1007/s00401-010-0779-6

[87] Cali I, Miller CJ, Parisi J, Geschwind M, Gambetti P, Schonberger L. Distinct pathological phenotypes of Creutzfelds-Jakob disease in recipients of prion-contaminated growth hormone. Acta Neuropathologica. 2015;**3**:37-46

[88] Apps R, Hawkes R. Cerebellar cortical organization: A one-map hypothesis. Nature Reviews. Neuroscience. 2009;**10**:670-681. DOI: 10.1038/nrn2698

[89] Reeber SL, White JJ, Georges-Jones NA, Sillitoe RV. Architecture and development of olivo-cerebellar circuit topography. Frontiers in Neural

Circuits. 2013;**6**:115. DOI: 10.3389/fncir.2012.00115

[90] Brochu G, Maler L, Hawkes R. Zebrin II: A polypeptide antigen expressed selectively by Purkinje cells reveals compartments in rats and fish cerebellum. The Journal of Comparative Neurology. 1990;**291**:538-552

[91] Armstrong R, Cairns N. Spatial patterns of the pathological changes in the cerebellar cortex in sporadic Creutzfeldt-Jakob disease (sCJD). Folia Neuropathologica. 2003;**41**:183-189

[92] Fujita H, Morita N, Furuichi T, Sugihara I. Clustered fine compartmentalization of the mouse embryonic cerebellar cortex and its rearrangement into the postnatal striped configuration. The Journal of Neuroscience. 2012;**32**:15688-15703. DOI: 10.1523/JNEUROSCI.1710-12.2012

[93] Zhou M, Ottenberg G, Sferrazza GF, Lasmézas CI. Highly neurotoxic monomeric alpha-helical prion protein. Proceedings of the National Academy of Sciences of the United States of America. 2012;**109**:3113-3118. DOI: 10.1073/pnas.1118090109

[94] Mallucci G, Ratte S, Asante EA, Linehan J, Gowland I, Jefferys JG, et al. Post-natal knock-out of prion protein alters hippocampal CA1 properties, but does not result in neurodegeneration. The EMBO Journal. 2002;**21**:202-210

[95] Halliday M, Radford H, Mallucci G. Prions: Generation and spread versus neurotoxicity. The Journal of Biological Chemistry. 2014;**289**:19862-19868

[96] Nakagawa T, Zhu H, Morishima N, Li E, Xu J, Bruce A, et al. Caspase-12 mediates endoplasmic reticulum-specific apoptosis and cytotoxicity by amyloid-β. Nature. 2000;**403**:98-103

[97] Hetz C, Russelakis-Carneiro M, Maundrell K, Castilla J, Soto C. Caspase-12 and endoplasmic reticulum stress mediate neurotoxicity of pathological prion protein. The EMBO Journal. 2003;**22**:5435-5445

[98] Soto C, Satani N. The intricate mechanisms of neurodegeneration in priondiseases. Trends in Molecular Medicine. 2011;**17**:14-24

[99] Mukherjee A, Morales-Scheihing D, Gonzalez-Romero D, Green K, Taglialatela G, Soto C. Calcineurin inhibition at the clinical phase of prion disease reduces neurodegeneration, improves behavioral alterations and increases animal survival. PLoS Pathogens. 2010;**6**:e1001138

[100] Sakudo A, Lee DC, Nakamura I, Taniuchi Y, Saeki K, Matsumoto Y, et al. Cell-autonomous PrP-Doppel interaction regulates apoptosis in PrP gene-deficient neuronal cells. Biochemical and Biophysical Research Communications. 2005;**333**:448-454

[101] Kurschner C, Morgan J. The cellular prion protein (PrP) selectively binds to Bcl-2 in the yeast two-hybrid system. Molecular Brain Research. 1995;**30**:165-168

[102] Kurschner C, Morgan J. Analysis of interaction sites in homo- and heteromeric complexes containing Bcl-2 family members and the cellular prion protein. Molecular Brain Research. 1996;**37**:249-258

[103] Laroche-Pierre S, Jodoin J, Leblanc A. Helix 3 is necessary and sufficient for prion protein's anti-Bax function. Journal of Neurochemistry. 2009;**108**:1019-1031

[104] Kuwahara C, Takeuchi AM, Nishimura T, Haraguchi K, Kubosaki A, Matsumoto Y, et al. Prions prevent

neuronal cell-line death. Nature. 1999;**400**:225-226

[105] Kim BH, Lee HG, Choi JK, Kim JI, Choi EK, Carp RI, et al. The cellular prion protein (PrPC) prevents apoptotic neuronal cell death and mitochondrial dysfunction induced by serum deprivation. Brain Research. Molecular Brain Research. 2004;**124**:40-50

[106] Bounhar Y, Zhang Y, Goodyer CG, LeBlanc A. Prion protein protects human neurons against Bax-mediated apoptosis. The Journal of Biological Chemistry. 2001;**276**:39145-39149

[107] Philot T, Drouet B, Pinçon-Raymond M, Vandekerckhove J, Rosseneu M, Chambaz J. A nonfibrillar form of the fusogenic prion protein fragment [118-135] induces apoptotic cell death in rat cortical neurons. Journal of Neurochemistry. 2000;**75**:2298-2308

[108] O'Donovan CN, Tobin D, Cotter TG. Prion protein fragment PrP-(106-126) induces apoptosis via mitochondrial disruption in human neuronal SH-SY5Y cells. The Journal of Biological Chemistry. 2001;**276**:43516-43523

[109] Lin D, Jodoin J, Baril M, Goodyer CG, Leblanc AC. Cytosolic prion protein is the predominant anti-Bax prion protein form: Exclusion of transmembrane and secreted prion protein forms in the anti-Bax function. Biochimica et Biophysica Acta. 2008;**1783**:2001-2012

[110] Giese A, Groschup MH, Hess B, Kretzschmar HA. Neuronal cell death in scrapie-infected mice is due to apoptosis. Brain Pathology. 1995;**5**:213-221

[111] Jesionek-Kupnicka D, Kordek R, Buczyński J, Liberski PP. Apoptosis in relation to neuronal loss in experimental Creutzfeldt-Jakob disease in mice. Acta Neurobiologiae Experimentalis. 2001;**61**:13-19

[112] Gray F, Chrétien F, Adle-Biassette H, Dorandeu A, Ereau T, Delisle MB, et al. Neuronal apoptosis in Creutzfeldt-Jakob disease. Journal of Neuropathology and Experimental Neurology. 1999;**58**:321-328

[113] Ferrer I. Synaptic pathology and cell death in the cerebellum in Creutzfeldt-Jakob disease. Cerebellum. 2002;**1**:213-222

[114] Drew SC, Haigh CL, Klemm HM, Masters CL, Collins SJ, Barnham KJ, et al. Optical imaging detects apoptosis in the brain and peripheral organs of prion-infected mice. Journal of Neuropathology and Experimental Neurology. 2011;**70**:143-150

[115] Cronier S, Carimalo J, Schaeffer B, Jaumain E, Béringue V, Miquel MC, et al. Endogenous prion protein conversion is required for prion-induced neuritic alterations and neuronal death. The FASEB Journal. 2012;**26**:3854-3861

[116] Sisó S, Puig B, Varea R, Vidal E, Acín C, Prinz M, et al. Abnormal synaptic protein expression and cell death in murine scrapie. Acta Neuropathologica. 2002;**103**:615-626

[117] Falsig J, Sonati T, Herrmann US, Saban D, Li B, Arroyo K, et al. Prion pathogenesis is faithfully reproduced in cerebellar organotypic slice cultures. PLoS Pathogens. 2012;**8**:e1002985

[118] Park SK, Choi SI, Jin JK, Choi EK, Kim JI, Carp RI, et al. Differential expression of Bax and Bcl-2 in the brains of hamsters infected with 263K scrapie agent. Neuroreport. 2000;**11**:1677-1682

[119] Coulpier M, Messiaen S, Hamel R, Fernández de Marco M, Lilin T, Eloit M. Bax deletion does not protect neurons from BSE-induced

death. Neurobiology of Disease. 2006;**23**:603-611

[120] Chiesa R, Piccardo P, Dossena S, Nowoslawski L, Roth KA, Ghetti B, et al. Bax deletion prevents neuronal loss but not neurological symptoms in a transgenic model of inherited prion disease. Proceedings of the National Academy of Sciences of the United States of America. 2005;**102**:238-243

[121] Heitz S, Lutz Y, Rodeau J-L, Zanjani H, Gautheron V, Bombarde G, et al. BAX contributes to Doppel-induced apoptosis of prion protein-deficient Purkinje cells. Developmental Neurobiology. 2007;**67**:670-686

[122] Selimi F, Doughty M, Delhaye-Bouchaud N, Mariani J. Target-related and intrinsic neuronal death in Lurcher mutant mice are both mediated by caspase-3 activation. The Journal of Neuroscience. 2000;**20**:992-1000

[123] Zanjani HS, Vogel MW, Martinou JC, Delhaye-Bouchaud N, Mariani J. Postnatal expression of Hu-bcl-2 gene in Lurcher mutant mice fails to rescue Purkinje cells but protects inferior olivary neurons from target-related cell death. The Journal of Neuroscience. 1998;**18**:319-327

[124] Fan H, Favero M, Vogel MW. Elimination of Bax expression in mice increases cerebellar Purkinje cell numbers but not the number of granule cells. The Journal of Comparative Neurology. 2001;**436**:82-91

[125] Zanjani HS, Vogel MW, Delhaye-Bouchaud N, Martinou JC, Mariani J. Increased cerebellar Purkinje cell numbers in mice overexpressing a human bcl-2 transgene. The Journal of Comparative Neurology. 1996;**374**:332-341

[126] Kim YS, Carp RI, Callahan SM, Wisniewski HM. Incubation periods and survival times for mice injected stereotaxically with three scrapie strains in different brain regions. The Journal of General Virology. 1987;**68**:695-702

[127] Zanjani HS, Vogel MW, Delhaye-Bouchaud N, Martinou JC, Mariani J. Increased inferior olivary neuron and cerebellar granule cell numbers in transgenic mice overexpressing the human Bcl-2 gene. Journal of Neurobiology. 1997;**32**:502-516

[128] Moore R. Proteomics analysis of amyloid and nonamylois prion disease phenotype reveals both common and divergent mechanisms of neuropathogenesis. Journal of Proteome Research. 2014;**13**:4620-4634

[129] Falsig J, Julius C, Margalith I, Schwarz P, Heppner FL, Aguzzi A. A versatile prion replication assay in organotypic brain slices. Nature Neuroscience. 2008;**11**:109-117

[130] Campeau JL, Wu G, Bell JR, Rasmussen J, Sim VL. Early increase and late decrease of Purkinje cell dendritic spine density in prion-infected organotypic mouse cerebellar cultures. PLoS One. 2013;**8**:e81776

[131] Wolf H, Hossinger A, Fehlinger A, Büttner S, Sim V, McKenzie D, et al. Deposition pattern and subcellular distribution of disease-associated prion protein in cerebellar organotypic slice cultures infected with scrapie. Frontiers in Neuroscience. Nov 4, 2015;**9**:410. DOI: 10.3389/frins.2015.00410

[132] Webb JL, Ravikumar B, Atkins J, Skepper JN, Rubinsztein DC. Alpha-Synuclein is degraded by both autophagy and the proteasome. The Journal of Biological Chemistry. 2003;**278**:25009-25013

[133] Pickford F, Masliah E, Britschgi M, Lucin K, Narasimhan R, Jaeger PA, et al. The autophagy-related protein

beclin 1 shows reduced expression in early Alzheimer disease and regulates amyloid beta accumulation in mice. The Journal of Clinical Investigation. 2008;**118**:2190-2199

[134] Xu Y, Tian C, Wang SB, Xie WL, Guo Y, Zhang J, et al. Activation of the macroautophagic system in scrapie-infected experimental animals and human genetic prion diseases. Autophagy. 2012;**8**:1604-1620

[135] Heitz S, Grant NJ, Leschiera R, Haeberlé AM, Demais V, Bombarde G, et al. Autophagy and cell death of Purkinje cells overexpressing Doppel in Ngsk Prnp-deficient mice. Brain Pathology. 2010;**20**:119-132

[136] Petersén A, Larsen KE, Behr GG, Romero N, Przedborski S, Brundin P, et al. Expanded CAG repeats in exon 1 of the Huntington's disease gene stimulate dopamine-mediated striatal neuron autophagy and degeneration. Human Molecular Genetics. 2001;**10**:1243-1254

[137] Nixon RA. Autophagy, amyloidogenesis and Alzheimer disease. Journal of Cell Science. 2007;**120**:4081-4091

[138] Spilman P, Podlutskaya N, Hart MJ, Debnath J, Gorostiza O, Bredesen D, et al. Inhibition of mTOR by rapamycin abolishes cognitive deficits and reduces amyloid-beta levels in a mouse model of Alzheimer's disease. PLoS One. 2010;**5**:e9979

[139] Yang DS, Stavrides P, Mohan PS, Kaushik S, Kumar A, Ohno M, et al. Therapeutic effects of remediating autophagy failure in a mouse model of Alzheimer disease by enhancing lysosomal proteolysis. Autophagy. 2011;**7**:788-789

[140] Heiseke A, Aguib Y, Riemer C, Baier M, Schätzl HM. Lithium induces clearance of protease resistant prion protein in prion-infected cells by induction of autophagy. Journal of Neurochemistry. 2009;**109**:25-34

[141] Cortes CJ, Qin K, Cook J, Solanki A, Mastrianni JA. Rapamycin delays disease onset and prevents PrP plaque deposition in a mouse model of Gerstmann-Sträussler-Scheinker disease. The Journal of Neuroscience. 2012;**32**:12396-12405

[142] Cuervo AM, Stefanis L, Fredenburg R, Lansbury PT, Sulzer D. Impaired degradation of mutant alpha-synuclein by chaperone-mediated autophagy. Science. 2004;**305**:1292-1295

[143] Chu C. Autophagic stress in neuronal injury and disease. Journal of Neuropathology and Experimental Neurology. 2006;**65**:423-432

[144] Kovacs G, Budka H. Prion diseases: From protein to cell pathology. The American Journal of Pathology. 2008;**172**:555-565

[145] Boelaard JW, Schlote W, Tateishi J. Neuronal autophagy in experimental Creutzfeldt-Jakob's disease. Acta Neuropathologica. 1989;**78**:410-418

[146] Dron M, Bailly Y, Beringue V, Haeberlé AM, Griffond B, Risold PY, et al. Scrg1 is induced in TSE and brain injuries, and associated with autophagy. The European Journal of Neuroscience. 2005;**22**:133-146

[147] Dron M, Bailly Y, Beringue V, Haeberlé A-M, Griffond B, Risold P-Y, et al. SCRG1, a potential marker of autophagy in transmisible spongiform encephalopathies. Autophagy. 2006;**2**:58-60

[148] Oh JM, Shin HY, Park SJ, Kim BH, Choi JK, Choi EK, et al. The involvement of cellular prion protein in the autophagy pathway in neuronal cells. Molecular and Cellular Neurosciences. 2008;**39**:238-247

[149] Doh-Ura K, Iwaki T, Caughey B. Lysosomotropic agents and cysteine protease inhibitors inhibit scrapie-associated prion protein accumulation. Journal of Virology. 2000;**74**:4894-4897

[150] Beranger F, Crozet C, Goldsborough A, Lehmann S. Trehalose impairs aggregation of PrPSc molecules and protects prion-infected cells against oxidative damage. Biochemical and Biophysical Research Communications. 2008;**374**:44-48. DOI: 10.1016/j.bbrc.2008.06.094

[151] Heiseke A, Aguib Y, Schätzl H. Autophagy, prion infection and their mutual interactions. Current Issues in Molecular Biology. 2010;**12**:11

[152] Yun SW, Ertmer A, Flechsig E, Gilch S, Riederer P, Gerlach M, et al. The tyrosine kinase inhibitor imatinib mesylate delays prion neuroinvasion by inhibiting prion propagation in the periphery. Journal of Neurovirology. 2007;**13**:328-337

[153] Aguib Y, Heiseke A, Gilch S, Riemer C, Baier M, Schätzl HM, et al. Autophagy induction by trehalose counteracts cellular prion infection. Autophagy. 2009;**5**:361-369

[154] Zhou M, Ottenberg G, Sferrazza GF, Hubbs C, Fallahi M, Rumbaugh G, et al. Neuronal death induced by misfolded prion protein is due to NAD+ depletion and can be relieved in vitro and in vivo by NAD+ replenishment. Brain. 2015;**138**:992-1008. DOI: 10.1093/brain/awv002

[155] Weissmann C, Flechsig E. PrP knock-out and PrP transgenic mice in prion research. British Medical Bulletin. 2003;**66**:43-60

[156] Criado JR, Sánchez-Alavez M, Conti B, Giacchino JL, Wills DN, Henriksen SJ, et al. Mice devoid of prion protein have cognitive deficits that are rescued by reconstitution of PrP in neurons. Neurobiology of Disease. 2005;**19**:255-265

[157] Oh JM, Choi EK, Carp RI, Kim YS. Oxidative stress impairs autophagic flux in prion protein-deficient hippocampal cells. Autophagy. 2018:1448-1461

[158] Shin HY, Park JH, Carp RI, Choi EK, Kim YS. Deficiency of prion protein induces impaired autophagic flux in neurons. Frontiers in Aging Neuroscience. 2014;**6**:207. DOI: 10.3389/fnagi.2014.00207

[159] Ko DC, Milenkovic L, Beier SM, Manuel H, Buchanan J, Scott MP. Cell-autonomous death of cerebellar purkinje neurons with autophagy in Niemann-pick type C disease. PLoS Genetics. 2005;**1**:81-95

[160] Sanchez-Varo R, Trujillo-Estrada L, Sanchez-Mejias E, Torres M, Baglietto-Vargas D, Moreno-Gonzalez I, et al. Abnormal accumulation of autophagic vesicles correlates with axonal and synaptic pathology in young Alzheimer's mice hippocampus. Acta Neuropathologica. 2012;**123**:53-70. DOI: 10.1007/s00401-011-0896-x

[161] Sakaguchi S, Katamine S, Nishida N, Moriuchi R, Shigematsu K, Sugimoto T, et al. Loss of cerebellar Purkinje cells in aged mice homozygous for a disrupted PrP gene. Nature. 1996;**380**:528-531

[162] Katamine S, Nishida N, Sugimoto T, Noda T, Sakaguchi S, Shigematsu K, et al. Impaired motor coordination in mice lacking prion protein. Cellular and Molecular Neurobiology. 1998;**18**:731-732

[163] Rossi D, Cozzio A, Flechsig E, Klein MA, Rulicke T, Aguzzi A, et al. Onset of ataxia and Purkinje cell loss in PrP null mice inversely correlated with

Dpl level in brain. The EMBO Journal. 2001;**20**:694-702

[164] Weissmann C, Aguzzi A. PrP's double causes trouble. Science. 1999;**286**:914-915

[165] Moore RC, Lee IY, Silverman GL, Harrison PM, Strome R, Heinrich C, et al. Ataxia in prion protein (PrP)-deficient mice is associated with upregulation of the novel PrP-like protein doppel. Journal of Molecular Biology. 1999;**292**:797-817

[166] Lu K, Wang W, Xie Z, Wong B-S, Li R, Petersen RB, et al. Structural characterization of the recombinant human doppel protein. Biochemistry. 2000;**39**:13575-13583

[167] Moore RC, Mastrangelo P, Bouzamondo E, Heinrich C, Legname G, Prusiner SB, et al. Doppel-induced cerebellar degeneration in transgenic mice. Proceedings of the National Academy of Sciences of the United States of America. 2001;**98**:15288-15293

[168] Lemaire-Vieille C, Bailly Y, Erlich P, Loeuillet C, Brocard J, Haeberlé AM, et al. Ataxia with cerebellar lesions in mice expressing chimeric PrP-Dpl protein. The Journal of Neuroscience. 2013;**33**:1391-1399

[169] Watts JC, Westaway D. The prion protein family: Diversity, rivalry, and dysfunction. Biochimica et Biophysica Acta. 2007;**1772**:654-672

[170] Heitz S, Gautheron V, Lutz Y, Rodeau JL, Zanjani HS, Sugihara I, et al. Bcl-2 conteracts Doppel-induced apoptosis of prion protein-deficient Purkinje cells in the Ngsk *Prnp*$^{0/0}$ mouse. Developmental Neurobiology. 2008;**68**:332-348

[171] Heitz S, Grant NJ, Bailly Y. Doppel induces autophagic stress in prion protein-deficient Purkinje cells. Autophagy. 2009;**5**:422-424

[172] Ding W, Yin X. Sorting, recognition and activation of the misfolded protein degradation pathways through macroautophagy and the proteasome. Autophagy. 2008;**16**:141-150

[173] Wang QJ, Ding Y, Kohtz DS, Mizushima N, Cristea IM, Rout MP, et al. Induction of autophagy in axonal dystrophy and degeneration. The Journal of Neuroscience. 2006;**26**:8057-8068

[174] Yue Z. Regulation of neuronal autophagy in axon: Implication of autophagy in axonal function and dysfunction/degeneration. Autophagy. 2007;**3**:139-141

[175] Yue Z, Friedman L, Komatsu M, Tanaka K. The cellular pathways of neuronal autophagy and their implication in neurodegenerative diseases. Biochimica et Biophysica Acta. 2009;**1793**:1496-1507

[176] Maday S, Wallace KE, Holzbaur EL. Autophagosomes initiate distally and mature during transport toward the cell soma in primary neurons. The Journal of Cell Biology. 2012;**196**:407-417

[177] Nixon RA, Yang DS, Lee JH. Neurodegenerative lysosomal disorders: A continuum from development to late age. Autophagy. 2008;**4**:590-599

[178] Fimia G, Piacentini M. Regulation of autophagy in mammals and its interplay with apoptosis. Cellular and Molecular Life Sciences. 2010;**67**:1581-1588. DOI: 10.1007/s00018-010-0284-z

[179] Metzger F, Kapfhammer JP. Protein kinase C: Its role in activity-dependent Purkinje cell dendritic development and plasticity. Cerebellum. 2003;**2**:206-214

[180] Dole S, Heitz S, Bombarde G, Haeberlé A-M, Demais V, Grant NJ, et al.

New insights into Doppel neurotoxicity using cerebellar organotypic cultures from prion protein-deficient mice. In: Medimond International Proceedings, Monduzzi Editors. Bologna Prion 2010, Salzburg, Austria. Sep 08-11, 2010. pp. 7-14